

On the Phase Behavior of Disordered Type-II Superconductors

Gautam I. Menon*

The Institute of Mathematical Sciences, C.I.T. Campus,

Taramani, Chennai 600 113, India

(December 2, 2024)

Abstract

A general phenomenology for phase behaviour in the mixed phase of disordered type-II superconductors is outlined. We propose that the “Bragg glass” phase generically transforms via two separate thermodynamic phase transitions into a disordered liquid on increasing the temperature. The first transition is into a glassy phase, topologically disordered at the largest length scales, but lacking the long-ranged phase correlations of a “vortex glass”. This phase has a significant degree of short-ranged translational order, unlike the disordered liquid, but no quasi-long range order, in contrast to the Bragg glass. This glassy phase, which we call a “multi-domain glass”, is confined to a narrow sliver at intermediate fields, but broadens out both for much larger and much smaller field values. Structure in the multi-domain glass is argued to resemble a disordered arrangement of crystalline domains. Estimates for typical domain sizes indicate that they can be far larger than the inter-line spacing for weak disorder, suggesting a plausible mechanism by which signals of a two-step transition can be obscured. Calculations of the Bragg glass-multi-domain glass and the multi-domain glass-disordered liquid phase

*Email:menon@imsc.ernet.in

boundaries are presented and compared to experimental data. We argue that these proposals provide a unified picture of the available experimental data on both high- T_c and low- T_c materials, simulations and current theoretical understanding.

PACS:74.60.-w,74.20.De,74.60.Ge,74.60.Jg,74.70.-b,74.72.-h

I. INTRODUCTION

In the mean-field phase diagram of a pure type-II superconductor, Meissner, mixed and normal phases are separated by continuous phase transitions associated with lower ($H_{c1}(T)$) and upper ($H_{c2}(T)$) critical fields [1]. In the mixed phase, an applied magnetic field H enters the sample in the form of singly quantized lines of magnetic flux. These lines repel each other, stabilizing a triangular line lattice. Thermal fluctuations melt this lattice via a first-order melting transition, subdividing the domain of the mixed phase into solid and fluid phases of flux lines [2–4].

With $\vec{H} = H\hat{z}$, flux-lines in the lattice phase are parametrized by two-dimensional coordinates \mathbf{R}_i , where \mathbf{R}_i describes the position of the i^{th} line. Deviations from this arrangement define a two-component displacement field $\mathbf{u}(\mathbf{R}_i, z)$, with an associated coarse-grained elastic free energy cost

$$F_{el} = \int d\mathbf{r}_\perp dz \left[\frac{c_{11}}{2} (\nabla_\perp \cdot \mathbf{u})^2 + \frac{c_{66}}{2} (\nabla_\perp \times \mathbf{u})^2 + \frac{c_{44}}{2} (\partial_z \mathbf{u})^2 \right]. \quad (1.1)$$

Here $\mathbf{u}(\mathbf{r}_\perp, z)$ is the displacement field at location (\mathbf{r}_\perp, z) . This term represents the elastic cost of distortions from the crystalline state, governed by the values of the elastic constants for shear (c_{66}), bulk (c_{11}) and tilt (c_{44}).

Quenched random pinning destabilizes the long-ranged translational order of the flux-lattice phase [1,5]. Such disorder adds

$$F_d = \int d\mathbf{r}_\perp dz V_d(\mathbf{r}_\perp, z) \rho(\mathbf{r}_\perp, z), \quad (1.2)$$

to F_{el} above, where F_d represents the interaction of vortex lines with a quenched disorder potential V_d and the density field $\rho(\mathbf{r}_\perp, z)$ is defined by

$$\rho(\mathbf{r}_\perp, z) = \sum_i \delta^{(2)}(\mathbf{r}_\perp - \mathbf{R}_i - \mathbf{u}(\mathbf{R}_i, z)). \quad (1.3)$$

If the disorder derives from a high density of weak, random point pinning sites, it is convenient to assume that V_d is drawn from a Gaussian distribution and is correlated over

a length scale ξ , the coherence length *i.e.* $[V_d(x)V_d(x')] = K(x - x')$, with $K(x - x')$ a short-ranged function of range ξ [5]. The notation x denotes (\mathbf{r}_\perp, z) .

Much theoretical attention has been devoted recently to the understanding of the statistical mechanics defined by Eqns.(1.1) and (1.2). The problem is the computation of correlation functions such as

$$B(\mathbf{r}_\perp, z) = [\langle \mathbf{u}(\mathbf{r}_\perp, z) - \mathbf{u}(\mathbf{0}, 0) \rangle^2], \quad (1.4)$$

where the brackets $\langle \cdot \rangle$ and $[\cdot]$ denote thermal and disorder averages respectively. At least two novel glassy phases arise as a consequence of such disorder [6–8]. In the relatively more ordered of these phases, the Bragg glass (BG) phase, correlations of the order parameter for translational correlations decay as power laws [7–12]:

$$C_{\mathbf{G}}(\mathbf{x}_\perp) = \overline{\langle \exp i[\mathbf{G} \cdot (\mathbf{u}(\mathbf{x}_\perp, z) - \mathbf{u}(\mathbf{0}, z))] \rangle} \sim 1/|\mathbf{x}_\perp|^{\bar{\eta}_G}, \quad (1.5)$$

where \mathbf{G} is a reciprocal lattice vector and $\bar{\eta}_G$ a non-universal exponent [11,12]. The anomalously large translational correlation lengths inferred from magnetic decoration experiments on BSCCO [13] and the resolution limited Bragg peaks obtained in neutron scattering from the mixed phase [14] in this material at small H , support the existence of a Bragg glass phase in type-II superconductors. Hall probe measurements [15] see a single first-order, temperature-driven melting transition out of the Bragg glass at such fields [14–17].

At increased levels of pinning, the Bragg glass is believed to be unstable to a disordered phase in which translational correlations decay exponentially at sufficiently large distances [9,10] *i.e.* $\lim_{x \rightarrow \infty} C_{\mathbf{G}}(\mathbf{x}) \sim \exp(-\mu|\mathbf{x}_\perp|)$. Such a phase *must* be separated by a phase transition from the Brass glass phase. At large H , experiments [18] indicate a continuous transition from an equilibrium fluid phase into a highly disordered glassy state when the temperature T is reduced from the mean-field $T_c(H)$ [19,20]. This disordered low- T , large- H state may be a new thermodynamic phase, the “vortex glass” (VG) phase, separated from the equilibrium disordered liquid (DL) by a line of continuous phase transitions [6]. However, the experiments may also be indicating a non-equilibrium regime [21]. A “frozen

liquid” similar to a structural glass and an “entangled liquid” analogous to a polymeric glass have been suggested as alternatives to the equilibrium vortex glass [21,22].

The phase diagram of Fig. 1 summarizes the currently popular view of the phase behaviour in the mixed phase of weakly disordered single crystals of anisotropic high- T_c systems such as BSCCO [9,16,17,20,23–25]. (This disorder is assumed to arise from a large density of weak point pinning sites in this paper [26].) Fig. 1 implies that the BG phase is unstable to the VG phase on increasing H . This feature follows from the belief that increasing H at a fixed level of microscopic disorder is equivalent to increasing the *effective* level of disorder [27]. Fig. 1 also shows the Bragg glass melting *directly* into the DL phase in the intermediate field regime (solid line). The VG to DL transition begins where the first-order BG-DL transition line terminates; this transition has been suggested to be continuous [17]. Recent Josephson plasma resonance experiments and magneto-optic studies in BSCCO [28,29] indicate that the underlying field-driven BG-VG transition may actually be a discontinuous one [30].

The importance of thermal fluctuations in the cuprates ensures that disordered phases such as the DL phase occupy much of the phase diagram in high- T_c materials [1]. In contrast, for most low- T_c systems, such disordered phases occupy a relatively small regime just below $T_c(H)$. The phase behaviour in the mixed phase of low- T_c superconductors has been the focus of recent attention [31–35]. These studies suggest a universal phase diagram for weakly pinned low- T_c type-II materials [35]. Interestingly, this phase diagram appears to differ significantly from Fig. 1.

The low- T_c systems studied have relatively large values of the Ginzburg number,

$$G_i = (k_B T_c / H_c^2 \epsilon \xi^3)^2 / 2, \quad (1.6)$$

which measures the relative importance of thermal fluctuations [1]. Here ξ is the coherence length, ϵ the mass anisotropy, T_c the superconducting transition temperature and H_c the thermodynamic critical field. In most low- T_c materials $G_i \sim 10^{-8}$, whereas $G_i \sim 10^{-2}$ for high- T_c superconductors such as $\text{YBa}_2\text{Cu}_3\text{O}_{7-\delta}$ (YBCO) and $\text{Bi}_2\text{Sr}_2\text{CaCu}_2\text{O}_{8+\delta}$ (BSCCO)

[1].

For the layered dichalcogenide 2H-NbSe₂ ($T_c \simeq 7.2\text{K}$), anisotropy, weak layering, small coherence lengths and large penetration depths enhance the effects of thermal fluctuations, yielding $G_i \sim 10^{-4}$ [36,37]. For the C15 Laves-phase superconductor CeRu₂ ($T_c \simeq 6.1\text{K}$), $G_i \sim 10^{-5}$ [38], while for the ternary rare-earth stannides Ca₃Rh₄Sn₁₃, ($T_c \simeq 8\text{K}$) and Yb₃Rh₄Sn₁₃, ($T_c \simeq 7.6\text{K}$) , $G_i \sim 10^{-7}$ [39–41]. For the quarternary borocarbide YNi₂B₂C ($T_c \simeq 15.5\text{K}$), $G_i \sim 10^{-6}$ [42]. These systems can be made relatively pure: the ratio of the transport critical current j_c to the depairing current j_{dp} ($j_{dp} = cH_c/3\sqrt{6}\pi\lambda$, with $H_c = \Phi_0/2\sqrt{2}\pi\lambda\xi$) in these low- T_c materials can be as small as 10^{-4} or 10^{-5} . For the high- T_c case, in contrast, $j_c/j_{dp} \sim 10^{-2}$. These values of G_i (1-4 orders of magnitude larger than for conventional low- T_c materials) and of j_c/j_{dp} imply that the phase behaviour of weakly pinned, low- T_c type-II superconductors can be studied using such compounds, in regimes where the phases and phase transitions discussed in the context of the cuprates are experimentally accessible.

Fig. 2 presents the proposal of this paper for a schematic phase diagram for weakly disordered type-II superconductors. This phase diagram incorporates and extends recent suggestions for the phase behaviour of low- T_c systems, proposed by this author and collaborators in Ref. [35]. It is argued that Fig. 2 should be a universal phase diagram for *all* disordered type-II superconductors, both low and high- T_c , in a sense made precise in this paper.

In Fig. 2, the term “multi-domain glass” describes the sliver of intermediate glassy phase, which we propose should generically intervene between BG and DL phases. This phase is argued to be a new *equilibrium* phase. The multi-domain glass at intermediate H connects smoothly to the highly disordered glassy state obtained at large H , the putative vortex glass. The term “multi-domain” focuses attention on the intermediate level of translational correlations obtained within this phase in the interaction dominated regime. Melting on T scans appears to occur discontinuously out of the MG at these field values [43,44]. Our MG phase is similar to the recently proposed “amorphous vortex glass” [23,45]. Like the

“phase-incoherent vortex glass” studied in detail in Ref. [11], our MG phase is topologically disordered at the largest length scales and should lack the long-ranged phase correlations which characterize the VG phase. However, we emphasize that spatial correlations in the MG phase can be fairly long-ranged, unlike correlations in typical amorphous phases and in the disordered liquid. In addition, the phase diagram we propose differs significantly from ones proposed in earlier work.

The multi-domain character of this phase is argued to manifest itself in the fact that the transition between BG and DL phases can occur via several intermediate stages, corresponding to the melting of different domains as a consequence of disorder-induced inhomogeneities in the melting temperature [46]. This can result in large noise signals [36] associated with a small number of fluctuators [36,47], intermediate structure in the ac susceptibility as a function of T [31,34], a stepwise expulsion of vortices [48], strong thermal instabilities [36,49] and a host of other phenomena specific to this phase [35], all features of the experimental data, which are hard to rationalize in other pictures.

We argue that the MG phase melts via a first-order phase transition to the DL phase on T scans at intermediate H . Fig. 2 shows this first-order transition line terminating [24] at a tricritical point, where it meets a (continuous) glass transition line. (This topology is suggested by many experiments [17]; however, recent experimental work, discussed in a later section, suggests a more complex topology, involving a critical end point, for the MG-DL transition line.) Some features of the phase diagrams proposed in Ref. [35] and in Fig. 2, notably the two-step character of the transition out of the BG phase in some regions of parameter space and the reentrant nature of the phase boundaries at low fields, were described in earlier work [31–34].

This paper addresses the following question: What links the phase behaviour of low and high- T_c systems? Physically, it is reasonable to expect that high- T_c and low- T_c superconductors should have *qualitatively* similar phase behaviour. (This expectation motivates some of the features of Fig. 2.) However, Figs. 1 and 2 have some qualitatively *different* features: Fig. 2 implies that the Bragg glass always melts directly into a disordered glassy phase upon

heating. This glassy phase is a continuation of the disordered phase obtained on cooling at high-field values. A subsequent transition, at intermediate H , separates the MG from the disordered liquid, as in Fig. 2. In contrast, consensus phase diagrams for high- T_c systems such as BSCCO and YBCO envisage at least one “multicritical point” (labelled (H_{cr}, T_{cr}) in Fig. 1) on the BG boundary in the $H - T$ plane. Below this point the BG melts directly into the disordered liquid [9,11,16,17,20].

This apparent distinction between the phase behaviour of low and high- T_c materials is surprising. This distinction is also manifest in the difference in phase behaviour exhibited by relatively pure samples of high- T_c materials which show an apparent multicritical point as discussed above, and somewhat more disordered samples. Even among the low- T_c systems, the data on relatively clean samples do not rule out a possible multicritical point, in contrast to the case for more disordered samples [34].

Thus, at least two possibilities suggest themselves. We refer to these as scenarios (1) and (2). In the first scenario, a genuine distinction exists between more disordered and less disordered samples, leading to the following picture for the experiments: If the disorder is sufficiently weak the sliver of MG phase vanishes altogether and the BG melts directly into the DL phase [50]. If the existence of a *low*-field glassy phase is assumed (as shown in Fig. 2), there should be two multicritical points on the BG-MG transition line, where the high-field and low-field glass transition lines meet the first-order BG-DL phase boundary. As disorder is increased, these two points approach each other on the BG-DL transition line. They then merge at a critical level of disorder. For stronger disorder, the BG-MG transition line splits off from the MG-DL transition line, the two glassy phases are linked smoothly and the phase diagram of Fig. 2 is obtained.

This scenario as well as the one outlined below *assume* the existence of a low-field glassy phase just above the lower critical field H_{c1} . Evidence for this phase is strongest in the low- T_c materials, in particular 2H-NbSe₂, [51] although there have been recent reports of similar low-field glassiness in the high- T_c material YBCO [52,53]. Both theoretically [54] and from the point of view of simulations [55], however, the possibility of a low-field glassy

phase appears to be fairly well established. Recent experiments indicate that the domain of this low-field glassy phase can extend far above H_{c1} in disordered samples of 2H-NbSe₂ [34,56]. In addition, the transition between the low-field glassy phase and the BG phase appears to be sharp [56].

The second scenario is the following: Any distinction between samples with different levels of disorder is only notional and the generic phase behaviour is that shown in Fig. 2 [57]. Thus, the BG phase would always be expected to transform first into a disordered MG phase and only then into the DL phase on T scans. It would then be necessary to rationalize the experimental observations of a possible single transition at intermediate H . *A-priori*, both scenarios are acceptable. However, they cannot both be correct *if* the phase diagram of a type-II superconductor with weak point pinning is universal.

In this paper, it is suggested that the second scenario is a theoretically attractive and experimentally viable alternative to the first. This paper discusses links between the phase diagrams of Figs. 1 and 2 in the context of the available experimental data, simulation results and theoretical understanding. The phase diagram of Fig. 2 is proposed to be the more basic one; Fig. 1 is argued to be recovered from Fig. 2 when the BG-MG and MG-DL transition lines shown in Fig. 2 come so close as to be separately unresolvable. (An alternative phase diagram which retains this feature but exhibits a more complex topology for the MG-DL transition line is discussed in a subsequent section.) It is argued that this is the case when thermal averaging over disorder is substantial, leading to an effective smoothening of the disorder potential. This discussion is motivated by the following conjecture for phase transitions out of the BG phase: *The BG phase is conjectured to always transform directly into the MG phase and never in a single step into the DL phase, at any finite level of disorder* [57]. Evidence from simulations, experiment and theory which supports this conjecture is discussed.

This paper contains six further sections. Section II summarizes the proposals of Ref. [35] for low- T_c systems and then supplements them with proposals appropriate for the description of high- T_c materials. Quantitative estimates are then provided in support of these

ideas. Sections III and IV describe a theoretical framework within which these proposals, particularly with regard to the phase boundaries, can be quantified – Section III discusses a Lindemann parameter-based approach to obtaining the phase boundary which separates BG from MG phases while Section IV discusses a semi-analytic approach to the MG-DL transition based on a replicated liquid state and density functional theory. Section V compares the predictions of these sections with experimental data, principally on low- T_c systems. Section VI discusses the proposals of Section II in the context of the experimental data on both high and low- T_c systems. The concluding section (Section VII) links these results with previous work and suggests several experiments which could explore the ideas described here.

II. UNIVERSAL PHASE DIAGRAM FOR DISORDERED TYPE-II SUPERCONDUCTORS

The proposals of Ref. [35] derived from an analysis of peak effect systematics in the low- T_c materials 2H-NbSe_2 , CeRu_2 , $\text{Ca}_3\text{Rh}_4\text{Sn}_{13}$, $\text{Yb}_3\text{Rh}_4\text{Sn}_{13}$ and $\text{YNi}_2\text{B}_2\text{C}$. Ref. [35], extending earlier work [34], pointed out that these systematics suggested a general link to an underlying *static* phase diagram. The peak effect (PE) itself refers to the anomalous *increase* in j_c seen close to $H_{c2}(T)$; this increase terminates in a peak, as H (or T) is increased, before j_c collapses rapidly in the vicinity of H_{c2} [58–60].

The results of Ref. [35] relating to the low- T_c materials studied there are summarized in the first three proposals listed below; the reader is referred to the original paper for more details. These proposals are extended to high- T_c systems in this paper. The approach is primarily phenomenological – it draws on published experimental data, simulations and theoretical input in attempting to describe a complete framework in which a large body of data on phase behaviour in the disordered mixed phase can be systematized and understood.

A. Proposals

1. The high-field “vortex glass” survives at intermediate field values as a sliver of disordered, glassy phase intervening between quasi-ordered (BG) and disordered liquid (DL) phases [35]. (We use the phrase “multi-domain glass” (MG) to describe both the intermediate sliver phase and the putative vortex glass phase to which it connects smoothly.) Thus, in going from Bragg glass to liquid on increasing the temperature at intermediate field values, two phase boundaries are generically encountered [31–33,61]. The first separates the BG phase from the MG phase while the second separates the MG phase from the DL phase [31–33,35]. At low field values, the BG-MG phase boundary is reentrant [2,51,54,55,62]. For materials with intermediate to high levels of disorder, the glass obtained at high field values is smoothly connected to the one obtained at low fields [35]. At low levels of disorder, the width of the sliver regime at intermediate fields is extremely narrow [31,34].
2. The sliver of glassy phase at intermediate field values defines the peak regime [36], the regime seen between the onset of the increase of the critical current j_c (at T_{pl} on temperature scans) and its peak value (at T_p on temperature scans) as functions of the applied field H and temperature T in materials which exhibit a sharp peak effect [34,35]. The dynamical anomalies seen in experiments in this regime (slow dynamics, history dependence, metastability, switching phenomena etc.) arise as a consequence of the static complexity of the underlying glassy state [35]. Linking these anomalies to an underlying equilibrium transformation of the flux-line system into a glassy state (*i.e.* the statics as opposed to the dynamics) suggests a simple and general solution of the problem of the origin of PE anomalies.
3. Structure in the sliver phase obtained at intermediate fields resembles a “multi-domain” structure, essentially an arrangement of locally crystalline domains [35]. The possibility of such an intermediate state is attractive because it represents a compromise between the relatively ordered lattice state and the fully disordered fluid. At the structural level, it is a “Larkin domain solid”, originally believed to represent the

fate of a crystal on the addition of quenched disorder [63]. This proposal rationalizes a large body of data on PE anomalies including “fracturing” of the flux-line array [33], the association of thermodynamic melting with the transition into the disordered liquid [43] as well as conjectures regarding the dynamic coexistence of ordered and disordered phases in transport measurements in the PE regime [64].

4. The transverse size of a typical domain R_D in such a “multidomain” structure can be much larger than the mean-interparticle spacing a . It is conjectured that R_D is bounded above by R_a , the length-scale at which thermal and disorder induced fluctuations of the displacement field (calculated within the BG phase) are of order a [24]. R_D is also conjectured to be *largest* in the intermediate-field, interaction-dominated regime but should decrease rapidly for much larger or smaller H , reflecting the increased importance of disorder both at high-field and low-field ends [34,35,51]. Similar statements should hold for the longitudinal sizes of such domains. In such a phase, translational correlations would be solid-like out to a distance of order R_D , but would decay rapidly thereafter. For sufficiently weak disorder, the size of a typical domain is large, reflecting the value of R_a . In contrast, in the DL phase significant spatial correlations exist only up to a few (1-2) intervortex spacings. Thus, the DL and MG phases at intermediate H should differ substantially at the level of local correlations for sufficiently weak disorder.
5. At intermediate values of H , the glassy phase to which the Bragg glass melts is confined to a narrow sliver which broadens out both at much larger and much smaller H . Thermal smoothening of disorder reduces the width of this sliver. It can render the sliver unobservable if the disorder is sufficiently weak, yielding an apparent single melting transition out of the ordered phase. This can happen for two reasons: First, domain sizes can be comparable to typical sample dimensions if the effective disorder is weak enough. Second, changes in critical currents signalling a transition between different phases can be too small to be resolvable; estimates also suggest that mag-

netization discontinuities across the BG-MG transition are very small. The apparent vanishing of the sliver explains the putative multicritical point [16,20] invoked in the context of phase diagrams for the mixed phase. While the sliver need not be resolvable in some classes of experiments which probe phase behaviour (for instance, it may not show up in dc magnetization measurements), it may be apparent in other experiments, particularly those which probe local correlations. For more disordered superconductors, whether of the high- T_c or low- T_c variety, a two-step transition should generically be seen.

6. A vortex glass phase of the type proposed by Fisher, Fisher and Huse does not exist. Gauge glass models for the VG transition do not show a finite T transition in three dimensions, once effects of screening are included [65]. Also, recent work questions earlier reports supporting a scaling description of the experimental data on disordered cuprates [66,67]. Theoretically, the evidence appears to favour a low-temperature glassy phase *without* long-ranged phase correlations, at least in the weak disorder limit [11]. It is thus unlikely that the glassy phase obtained at low temperatures and elevated field values is a true phase-coherent vortex glass, in the sense of the original proposal [11]. However, many experiments in the peak effect regime of low and high- T_c materials show that the multi-domain glass which intervenes between the BG and the DL phases has strongly glassy properties [31,32,36,47,68–70]. The data on low- T_c systems favours an equilibrium transition [35] for the following reasons: (i) the approach to the intermediate regime is discontinuous and the phase boundaries reproducible, (ii) behaviour in this regime is dynamically very anomalous and, (iii) this phase connects smoothly to the high-field (VG) phase, argued extensively to be glassy in nature. This suggests that the intermediate multi-domain glass is a true equilibrium glassy phase for reasons which may have nothing to do with the original vortex glass proposal. The precise nature of the symmetry breaking which distinguishes the MG phase from the DL phase is at present unclear [71].

7. As a consequence of such glassiness, a hierarchy of long-lived metastable states can be obtained over significant parts of the phase diagram, leading to slow and non-trivial relaxation behaviour [68,72]. Such states may dominate the experimentally observed behaviour at low temperatures and high fields and mimic the behaviour expected of an equilibrium vortex glass phase. As a further corollary, experiments at low temperature and high field values may often be probing strongly non-equilibrium behaviour, once time-scales for structural relaxation exceed experimental time-scales, thereby obscuring the underlying *equilibrium* phase transitions.

B. Evidence for a Multi-domain state in the MG phase

A substantial body of data favours a multi-domain structure in the regime intermediate between BG and DL phases. A representative cross-section of this evidence is presented here.

Recent neutron scattering measurements on disordered single crystals of Niobium ($H_{c2}(4.2K) = 4.23 \text{ kOe}$, $T_c(0) \simeq 9K$), which show a sharp peak effect, suggest fairly ordered crystal-like states obtained by heating following cooling in zero field, even for temperatures in the regime between T_{pl} (T_o in Ref. [73]) and T_p , the “peak regime” [73]. Following Ref. [35], this regime defines the sliver of MG phase which intervenes between BG and DL phases at intermediate H . In contrast, the metastable disordered states obtained by field-cooling through the peak regime show nearly isotropic rings of scattering, indicating relatively short translational correlation lengths, comparable to those in a disordered liquid state. Experiments see a 30% reduction in rocking curve widths of Bragg spots between field cooled (FC) and zero-field cooled (ZFC) configurations demonstrating a fair degree of local order in the latter. That the relatively ordered states in the peak regime obtained on zero field cooling are actually lower in free energy can be demonstrated through experiments in which field-cooled states below T_p are annealed through the application of an ac field [73]. These data are consistent with SANS data on 2H-NbSe₂ [49].

Recent muon-spin rotation experiments [74,75] on BSCCO show a narrow intermediate phase where the asymmetry parameter associated with the field distribution function $n(B)$,

$$\alpha = \langle \Delta B^3 \rangle^{1/3} / \langle \Delta B^2 \rangle^{1/2}, \quad (2.1)$$

where $\Delta B = B - \langle B \rangle$, jumps from a value of $\alpha \sim 1.2$ at low T to a somewhat smaller value $\alpha \sim 1$ before a further jump to a value close to zero [74] at the irreversibility line. Large values of this asymmetry ($\alpha \sim 1.2$) indicate a fairly well-ordered lattice structure, while values close to zero indicate a highly symmetric arrangement of vortices, as in a liquid. The observation of such asymmetric linewidths in this narrow intermediate phase can be associated to the multidomain structure of the sliver of MG phase expected to intervene between BG and DL phases. These results would suggest a structure with a fair degree of local order, sufficiently different from the disordered liquid.

As T is raised further, individual domains can melt due to disorder induced variations in the local melting temperature T_M , leading to a mosaic of solid-like and liquid-like (amorphous) domains, similar to a regime of two-phase coexistence. This picture rationalizes several observations in the literature. Experiments on YBCO find that the magnetization discontinuities and first-order behaviour associated with the melting transition in the interaction dominated regime at intermediate H can be associated with the *MG-DL* transition at higher fields, once the BG-MG line splits off from the putative multicritical point [76,77]. In addition, there appears to be a critical point on this first-order line, beyond which these discontinuities vanish. The idea that structure similar to two-phase coexistence may account for some properties of the vortex array just below the melting transition has been raised in earlier work [78,79].

These features are easily explained within the picture outlined here. The melting transition in this scenario should generically be associated with the MG-DL shown in Fig. 2, although the finite width of the sliver regime implies that some part of the discontinuity in density between fluid and solid phases can be absorbed across the width of the sliver [35]. If R_D , the characteristic domain size, is of order or smaller than the translational correlation

length at freezing ξ_M , sharp signals of melting are no longer expected [27]. On the other hand, if $R_D \gg \xi_M$ at the melting transition, the behaviour should be equivalent to that of the pure system. Assuming $R_D \gg \xi_M$ initially, as R_D decreases on an increase in H (proposal (4) and the results of Refs. [24,45]) it approaches ξ_M ; the point where $R_D \simeq \xi_M$ defines the point where magnetization discontinuities should cease to be seen and thus the experimentally observed critical point.

The possibility that the vortex glass phase obtained from the BG phase on *field* scans might have a relatively low equilibrium density of dislocations was proposed recently by Kierfeld and Vinokur to rationalize some of the anomalies mentioned above [24]; related ideas in the low- T_c context appeared in Ref. [31]. We argue here that such a picture is also applicable to the *temperature*-driven transition out of the BG phase, as is clear from Fig. 2.

Hypothesizing such a multi-domain in the intermediate sliver regime is consistent with the suggestion that a “fracturing transition” from a solid with quasi-long-range order into a intermediate state with correlation lengths of some tens of interparticle spacings is responsible for the unusual open hysteresis loops obtained on thermal cycling within the peak effect regime in 2H-NbSe₂ [31]. The idea that the regime which interpolates between the low-temperature ordered phase and the high-temperature disordered phase might have a relatively large degree of translational order has been used to rationalize the difference in behavior of the ac susceptibility in ZFC and FC scans in studies of the peak effect in several low- T_c materials [33].

A fourth piece of evidence favouring a multi-domain or “fractured” state comes from voltage noise measurements, as pointed out in Ref. [35]. Experiments see a substantial enhancement in noise within the peak regime [47,69], a feature also seen in the ac susceptibility noise [33]. This noise is profoundly non-Gaussian in a regime where the PE is strongest; the number of independent fluctuators contributing to this noise turns out to be small [47]. Experiments indicate a possible static origin for this noise, as opposed to a purely dynamic origin such as the interaction of fluctuating flow channels [47]. This supports a picture of domains of mesoscopic size *in equilibrium* with each domain an “independent fluctuator”

contributing to the noise.

Recent simulation work on a pancake vortex model [80] indicates that the PE may be associated primarily with a *decoupling* transition in the c-axis direction, in which c-axis correlations of vortices become short-ranged. This author and collaborators have argued recently that modelling the MG phase in a pancake vortex model in terms of a random stacking of perfectly crystalline layers should yield a fairly high-energy situation, with an energy which scales linearly with the area of each plane [21]. It is reasonable that some fraction of this cost can be relaxed by allowing dislocations to enter into each layer, leading to a situation far more like the “multidomain” structure proposed in this paper than a decoupled pancake-vortex state [21,19].

Other simulations, such as those of van Otterlo *et. al.* [81,82] are consistent with an intermediate field MG phase with a correlation length intermediate between the solid and the disordered liquid. These simulations see primary peaks in the structure factor appropriate to the MG phase which transform into rings only across a second transition into the DL phase. The existence of these peaks indicates a fair degree of translational order, comparable to the sizes of the system studied, although the dynamics changes abruptly across the BG-MG transition. Interestingly, van Otterlo *et. al.* conclude that they cannot rule out the existence of a sliver of MG phase always preempting a direct BG-DL transition [35].

C. Domain Sizes in the MG phase

The scale for R_a is itself set by a combination of the Larkin pinning length scale, at which disorder and thermal fluctuation induced displacements are of order ξ , as well as the inter-line spacing a [1,11]. These can be derived from $B(\mathbf{r}_\perp, z)$. The transverse Larkin pinning length R_p is defined through $B(R_p, 0) \simeq \xi^2$. A second length-scale, the longitudinal Larkin pinning length L_p^b , is defined through $B(0, L_p^b) \simeq \xi^2$. At transverse (longitudinal) length scales of order R_p (L_p^b), the disorder-induced wandering of the displacement field equals the size of a pinning centre (ξ) at $T = 0$. A third important (transverse) length scale is the

scale R_a at which disorder and thermal fluctuation induced displacements in the direction transverse to the field become of order the inter-line spacing a : $B(R_a) \simeq a^2$.

At finite temperatures, replacing ξ^2 by $\max(\xi^2, \langle u^2 \rangle)$ in the equations defining L_p and R_p above defines length scales L_c^b and R_c . Here $\langle u^2 \rangle$ is the square of a “Lindemann length”; these quantities are directly related to the critical current. In the Bragg glass, $B(r)$ shows the following properties: For $r_\perp, z \ll R_c, L_c^b$, correlations behave as in the Larkin “random force” model *i.e.* $B(x) \sim x^{4-d}$. At length scales between R_c and R_a (the scale at which disorder-induced positional fluctuations become of order a), the random manifold regime, $B(x) \sim x^{2\zeta_{rm}}$. The exponent $\zeta_{rm} \sim (4-d)/6 \sim 1/6$. At still larger length scales, $B(x) \sim \log(x)$, yielding an asymptotic power law decay of translational correlations [7–9,11].

The Larkin length scales R_p and L_c^b and the Larkin volume $V_c \sim R_c^2 L_c^b$ are estimated as [1] $L_c^b = 2\xi^2 c_{66} c_{44} / n f^2$ and $R_c = \sqrt{2} \xi^2 c_{66}^{3/2} c_{44}^{1/2} / n f^2$. Using these, the standard weak-pinning expression for the critical current density j_c follows [1]:

$$j_c = \frac{1}{B} f \left(\frac{n}{V_c} \right)^{1/2}. \quad (2.2)$$

R_c and L_c^b for a relatively clean 2H-NbSe₂ single crystal are estimated in the following way [1]. We anticipate that the following condition is satisfied: $R_c, L_c^b > \lambda$, implying that non-dispersive ($k = 0$) values of the elastic constants can be used in our estimates. Then,

$$j_c \sim \left(\frac{\xi}{R_c} \right)^2 j_{dp}, \quad (2.3)$$

$$L_c^b \sim \frac{\lambda}{a} R_c. \quad (2.4)$$

Assuming values of $T_c \simeq 7K$, $\lambda \simeq 700\text{\AA}$ ($H \parallel c$), $\xi \sim 70\text{\AA}$ and a flux-line spacing $a (= \sqrt{2\Phi_0/\sqrt{3}B}) \sim 450\text{\AA}$ at $B \sim 1T$. For $10^{-4} < j_c/j_{dp} < 10^{-6}$, we then obtain:

$$\frac{R_c}{a} \sim \begin{cases} 150 & (j_c/j_{dp} = 10^{-6}); \\ 15 & (j_c/j_{dp} = 10^{-4}) \end{cases} \quad (2.5)$$

and

$$\frac{L_c^b}{a} \sim \begin{cases} 240 & (j_c/j_{dp} = 10^{-6}); \\ 24 & (j_c/j_{dp} = 10^{-4}) \end{cases} \quad (2.6)$$

The domain size R_D has been conjectured above (see proposal (4)) to be of order R_a in the intermediate H , interaction dominated regime. R_a is estimated via

$$R_a \simeq R_c \left(\frac{a}{\xi}\right)^{1/\zeta_{rm}}, \quad (2.7)$$

where R_c is the (transverse) Larkin pinning length scale [8,9,11]. At typical laboratory fields $\sim 1T$, we estimate

$$\left(\frac{a}{\xi}\right)^{1/\zeta_{rm}} \sim \left(\frac{450}{70}\right)^6 \sim 7 \times 10^4. \quad (2.8)$$

This leads to

$$10^5 \leq R_a/a \leq 10^6, \quad (2.9)$$

for a system with the parameter values described above. These are *overestimates*; allowing for the wave-vector dependence of elastic constants and prefactors neglected in these simple order-of-magnitude estimates should reduce these numbers considerably, possibly by factors of 10 or more.

Assuming a multi-domain structure within the peak regime, a typical scale for each domain of $R_a \sim 10^4 a$, $a \sim 400 \text{ \AA}$ at $H \sim 1T$ and a (longitudinal) Larkin length comparable to the size of the sample in the c-axis direction, one can obtain an estimate for the number of “independent fluctuators” discussed above in the context of the noise measurements. For a crystal of typical transverse area $A \sim 1 \text{ mm} \times 1 \text{ mm} \sim 10^{14} \text{ \AA}^2$ the number of such fluctuators N_f is estimated as

$$N_f = \frac{A}{A_D} \sim 10^1 - 10^2, \quad (2.10)$$

numbers small enough to yield the strong non-Gaussian effects seen in the experiments, particularly if one assumes that not all domains are active contributors to the noise signal.

Thermal fluctuations smear the effective disorder potential seen by a vortex line. If the thermally induced fluctuation of a vortex line about its equilibrium position exceeds ξ , the

effective pinning potential seen by a pinning site is strongly renormalized. An estimate of this effect at the level of a single pinned line [54] yields

$$U_p \sim U_p(0) \exp[-c(T/T_{dp})^3], \quad (2.11)$$

where $U_p(0)$ is the pinning potential associated with a single pinning site at $T = 0$, c is a numerical constant and T_{dp} is a characteristic temperature scale, the depinning temperature.

The value of the depinning temperature T_{dp} can be estimated from

$$T_{dp} \sim (U_p^2 \xi^3 c \epsilon_0 / \gamma^2)^{1/3}. \quad (2.12)$$

U_p is a measure of the pinning energy per unit length, ϵ_0 is the line tension of a single vortex, c is a numerical constant of order unity and γ is the mass anisotropy. Independent measures yield $T_{dp} \sim 25 - 40K$ for YBCO [22,23,76].

The ratio $R = T_{dp}^{low}/T_{dp}^{high}$ is then a quantitative measure of the relative importance of thermal fluctuations in low and high T_c materials. We use the following values:

$$NbSe_2 : U_p = 10K/\text{\AA}, \xi = 70\text{\AA}, \lambda = 700\text{\AA}, \gamma = 5 \quad (2.13)$$

and

$$YBCO : U_p = 10K/\text{\AA}, \xi = 20\text{\AA}, \lambda = 1400\text{\AA}, \gamma = 50, \quad (2.14)$$

and obtain $R \sim 10^2$, suggestive of the relative importance of this effect to the high- T_c materials *vis a vis* its irrelevance in low- T_c systems except very close to H_{c2} . A more accurate estimate of the magnitude of this effect comes from computing the ratio

$$R \frac{T_m^{high}}{T_m^{low}} \sim R \frac{T_c^{high}}{T_c^{low}} \sim 10^3, \quad (2.15)$$

where T_m is the melting temperature of the pure flux-line lattice and we have approximated $T_m \sim T_c$ in both cases.

That thermal fluctuations lead to a substantial reduction in the effectiveness of disorder close to the melting line in YBCO and BSCCO is clearly evident from experimental

measurements of the irreversibility line in single crystals of these materials [76,77,86]. The irreversibility line at intermediate fields ($H \sim 3 - 7T$) in YBCO actually appears to lie well *below* the melting line in weakly disordered samples [76]. Thus, thermal melting occurs in the almost totally reversible regime. Precision measurements [87] reveal a weak residual irreversibility, with attendant j_c values close to the melting transition of about $0.4A/cm^2$, comparable to that obtained in the purest samples of 2H-NbSe₂, but at much larger temperatures; $T_m \sim 80K$ in YBCO at $H \sim 5T$, compared to T_c 's of about 7K for 2H-NbSe₂. Similiar results have been obtained for BSCCO at fields less than about 0.05T [88]. In contrast, experiments on the low- T_c materials discussed in Refs. [34,35] indicate an irreversibility line which lies *above* both T_p and T_{pl} lines, and subdivides the disordered liquid further into irreversible and irreversible liquid regimes. In these systems, the evidence for a two-step transition appears unambiguous.

Such anomalously *small* values of j_c (j_c is proportional to the width of magnetic hysteresis loops and vanishes in the perfectly reversible regime), should lead to anomalously *large* values of R_c . Using $j_c/j_0 \sim 10^{-7}$, and ξ and λ values appropriate to YBCO, yields a characteristic domain size of order 1mm, clearly comparable to typical sample dimensions. Although these estimates are approximate ones, the physical intuition should be robust: characteristic domain sizes associated with an intermediate MG phase in high- T_c materials can be fairly large. Accordingly, in relatively pure samples of a small size, only a single sharp melting transition may be obtained, justifying the putative multicritical point and the direct transition into the liquid phase obtained in some measurements.

The estimates above indicate that the length R_a can be far larger than typical correlation lengths in the disordered fluid at the melting transition $\xi_M \sim 2 - 3a$. SANS experiments on Nb indicate translational correlations of this order [73]. Thus sharp signals of melting can be expected at the second transition line intersected on a T scan out of the BG phase; such signals should cease when $R_D \sim \xi_M$.

The phase boundary between a multidomain solid and the disordered liquid can thus be argued on physical grounds to have a critical point. This is analogous to the gas-liquid

transition in the following way: There is no symmetry distinction at the *structural* level between a multi-domain state and a DL phase; the multi-domain solid has neither long-ranged crystalline order nor the power-law correlations of a Bragg glass. However, if a thermodynamic transition into a glassy phase with a symmetry different from that of the DL (or multi-domain state) exists, the associated phase boundary cannot terminate except at $T = 0$ or *on* another phase transition line. Fig. 2 accounts for such an equilibrium glass transition. The topology of the MG-DL phase boundary is consistent with recent experimental work on single crystals of YBCO [76] and data on low- T_c systems [34,35]. However, no arguments appear to rule out alternative locations for this line of glass transitions such as the one proposed in recent simulation work [30] or more complex topologies, such as a critical end-point for the MG-DL transition line.

III. BG-MG PHASE BOUNDARY FROM A LINDEMANN PARAMETER APPROACH

The field-driven BG-MG transition occurs even at $T = 0$, where it is driven solely by changing the effective disorder. It represents a transition into a multidomain state at intermediate H on T scans. Such a state is substantively different from the equilibrium disordered fluid in terms of its local correlations and average density, provided the disorder is sufficiently weak. In contrast, the second transition, between MG and DL phases, is a close relative of thermal melting in the pure system.

The simplest way to estimate phase boundaries such as those shown in Figs. 1 and 2 uses a Lindemann-parameter based approach. The treatment of the BG-MG transition line described here uses arguments similar to those of Giamarchi and Le Doussal (GLD) [9,17]. It differs from their approach in the following way: GLD study this transition only at $T = 0$ (where thermal fluctuations are absent) and at high temperatures where it is argued that disorder can be neglected and an expression for the melting line in the pure system used. The calculation here studies the crossovers in detail in the context of the experimental

data on the low- T_c systems analysed in Ref. [35]. A more substantial difference between this approach and that of GLD is the proposal here that the high-temperature intermediate field transition out of the Bragg glass is *not* equivalent to thermal melting but rather to a transition to an intermediate ‘multi-domain state’ with the properties discussed in the previous section.

A convenient phenomenological characterization of the melting transition in simple three-dimensional solids indicates that the transition occurs when the root mean-square fluctuation of an atom from its equilibrium position equals a given fraction (c_L , the Lindemann parameter) of the interatomic spacing a . Giamarchi and Le Doussal suggested a possible generalization of this idea to the study of the instabilities of the Bragg glass phase [9]. Taking over their proposal, we compute the ratio

$$B(r_\perp = a)/a^2 = c_L^2, \quad (3.1)$$

(see Eq.1.4), to obtain the melting line taking c_L to be a universal number independent of H and T .

In the random manifold regime, using a variational replica symmetry breaking ansatz, GLD derive the following relation

$$B(r_\perp) = \frac{a^2}{\pi^2} \tilde{b}(r_\perp/R_a), \quad (3.2)$$

where the crossover function

$$\tilde{b}(x) \sim 1, \quad x \rightarrow 1, \quad (3.3)$$

and

$$\tilde{b}(x) \sim x^{1/3}, \quad x \rightarrow 0. \quad (3.4)$$

In a calculation which assumes wave-vector independent elastic constants, GD obtain R_a as

$$R_a = \frac{2a^4 c_{66}^{3/2} c_{44}^{1/2}}{\pi^3 \rho_0^3 U_p^2 (2\pi\xi^3)}. \quad (3.5)$$

Here c_{44} is the tilt modulus of the flux-line system and c_{66} its shear modulus, both calculated at zero wave vector. U_p measures the pinning strength per unit length, a is the mean intervortex spacing and ρ_0 is the areal density of vortices given by $\rho_0 = B/\Phi_0$, with Φ_0 the flux quantum: $\Phi_0 = 2.07 \times 10^{-15} T m^2$. It is assumed that $H \gg H_{c1}$, so that the effects of bulk distortions can be neglected.

These expressions can be used to derive the full BG-MG transition line in the H - T plane. For weak disorder, $R_a \gg a$. The following expressions for the elastic constants are used:

$$c_{66} = \frac{\epsilon_0}{4a^2} (1 - B/B_{c2}(T))^2, \quad (3.6)$$

and

$$c_{44} = \frac{B^2}{4\pi} \frac{(1 - B/B_{c2}(T))}{B/B_{c2}(T)}. \quad (3.7)$$

Here $\epsilon_0 = (\Phi_0/4\pi\lambda^2)$. The effects of a wave-vector dependent elasticity have been approximately accounted for in writing these expressions. Note that the elastic constants vanish as $B \rightarrow B_{c2}(T)$; at lower fields the expression for c_{66} should include a contribution from the line tension of isolated flux lines, which is neglected here.

Some algebra then yields the intermediate expression

$$c_L^2 = \frac{1}{a^{2/3}} \lambda(T) \frac{[B/B_{c2}(T)]^{1/6}}{[1 - B/B_{c2}(T)]^{7/6}} \frac{1}{\Phi_0^{4/3}} (U_p^{2/3} \xi) \times N, \quad (3.8)$$

where N is a numerical factor.

To simplify $U_p^{2/3} \xi$, we use the “core pinning” assumption

$$U_p = p \frac{H_c^2}{8\pi} \xi^2, \quad (3.9)$$

where p is a constant of order 1. This models the sources of pinning disorder as small-scale point defects on the scale of ξ , which act to reduce T_c locally. Using

$$H_c = \Phi_0 / (2\sqrt{2}\pi\xi\lambda), \quad (3.10)$$

leads to

$$U_p^{2/3}\xi = \frac{\Phi_0^{4/3}}{(2\sqrt{(2)\pi})^{4/3}} \left(\frac{p}{8\pi}\right)^{2/3} \frac{1}{\kappa} \frac{1}{\lambda^{1/3}}, \quad (3.11)$$

Defining $b = B/B_{c2}(T = 0)$ and assuming a temperature independent $\kappa (= \lambda/\xi)$, considerable algebra then yields the implicit expressions for the transition line $b(t)$ given below, given the following assumptions about the temperature dependence of the penetration depth λ and the upper critical field H_{c2} :

1. Assuming a temperature dependence of λ of the phenomenological two-fluid type *i.e.*

$$\lambda = \lambda(T = 0)/(1 - t^4)^{1/2}, \quad (3.12)$$

where $t = T/T_c(H = 0)$ and a linear dependence of $B_{c2}(T)$, *i.e.*

$$B_{c2}(T) = B_{c2}(0)(1 - t), \quad (3.13)$$

yields the relation:

$$\Sigma = \frac{b^3(1 - t)^6}{(1 - t^4)^2(1 - t - b)^7}. \quad (3.14)$$

Here Σ is assumed to be constant; its value involves the product of the Lindemann parameter c_L , κ , and p in the following ratio: $c_L^{12}\kappa^2/p^4$, multiplied by a numerical constant of value 1.88×10^7 . Assuming $\kappa \sim 1$, $c_L \sim 0.22$ and $p \sim 1$, yields $\Sigma \sim 0.25$. However, Σ is very sensitive to the value of c_L used; changing c_L by a factor of 2 to 0.11 changes Σ by a factor of about 5×10^{-3} . For $c_L = 0.15$, $\kappa = 1$ and $p = 1$, we obtain $\Sigma = 0.002$. For this reason, we use Σ as a fitting parameter and consider values for it in the range $10^{-3} < \Sigma < 10^2$.

Eq. (3.14) is plotted in Fig. 3, for different values of Σ , in the range $0.01 < \Sigma < 60$; the MG phase lies above these lines while the BG phase lies below them. Note that the transition lines are almost linear in $(1-t)$ for large values of Σ .

2. Assuming a temperature dependence of λ of the phenomenological two-fluid type *i.e.*

$$\lambda = \lambda(T = 0)/(1 - t^4)^{1/2}, \quad (3.15)$$

where $t = T/T_c(H = 0)$ and a quadratic dependence of $B_{c2}(T)$, *i.e.*

$$B_{c2}(T) = B_{c2}(0)(1 - t^2), \quad (3.16)$$

yields:

$$\Sigma = \frac{b^3(1 - t^2)^6}{(1 - t^4)^2(1 - t^2 - b)^7}. \quad (3.17)$$

Again, the numerical value of Σ is dictated essentially by the value of c_L ; we choose a similar range of Σ values as in the previous case. This relation is plotted in Fig. 4, for different values of Σ , in the range $0.01 < \Sigma < 50$. These plots show a more substantial curvature than the analogous plots for case (1) above.

In addition, assuming a temperature dependence of λ of the following linear type $\lambda = \lambda(T = 0)/(1 - t)^{1/2}$ where $t = T/T_c(H = 0)$ and a linear dependence of $B_{c2}(T)$, *i.e.* $B_{c2}(T) = B_{c2}(0)(1 - t)$ yields $\Sigma'' = \frac{b^2(1-t)^5}{(1-t-b)^7}$. This parametrization yield a BG-MG phase boundary which is virtually a straight line, for the range of Σ values displayed in Figs. 3 and 4. Note that all these results use different approximate parametrizations of $B_{c2}(T)$; the parametrizations involved in Eqs.(3.14) and (3.17) are both commonly found in the literature. Whether one or the other expression should be used should depend on the quality of fits to the experimentally obtained $B_{c2}(T)$ line. We use the first parametrization for the 2H-NbSe₂ data (Section V), but the second parametrization for both the CeRu₂ and the Ca₃Rh₄Sn₁₃ data discussed in that section.

For the phase boundaries to be physical, $t+b$ must be less than or equal to 1. We perform the computations using Eq.(3.14). One point on the curve is $(b = 0, t = 1)$; b increases monotonically with $1 - t$. At $t = 0$, the critical value of the magnetic field separating the BG phase from the MG phase satisfies $\frac{b(0)^3}{(1-b(0))^7} = \Sigma$. For Σ small $b(0) \sim \Sigma^{1/3}$, while for

large Σ , $b(0) \sim 1 - 1/\Sigma^{1/7}$ The shape of the $b - t$ phase diagram close to $b = 0$ is also easily obtained. For $t \rightarrow 1$, we have $b \sim (1 - t)$.

These calculations use a simple analytic parametrization of correlation functions in the BG phase, obtained after many further approximations on an initially simplified Hamiltonian, together with the restriction to a constant (field and temperature independent) Lindemann parameter. As a consequence, the quantitative predictions of this section should not be taken excessively seriously. However, the qualitative trends in the data appear to be borne out in this scheme of calculation, as discussed further in Section V.

IV. SEMI-ANALYTIC CALCULATION OF THE MG-DL TRANSITION LINE

This section discusses a calculational approach to the MG-DL phase boundary. The method outlined here uses results from a replica theory proposed by this author and Dasgupta (Ref. [27]) for the correlations of a vortex liquid in the presence of random point pinning [19]. This work examined the instability, within mean-field theory, of the DL phase to a crystalline state.

The estimates obtained above indicated that typical domain sizes in the MG phase, could be much larger than the translational correlation length at freezing in systems with low levels of pinning. In addition, the transition out of the DL phase at intermediate H appears experimentally to be first order. A natural first approximation is to analyse, in mean-field theory, the instability of the liquid to an ordered crystalline state. This approach should thus represent the physics of the first-order part of the MG-DL transition line in the interaction dominated regime at intermediate H . The issue of the nature of glassiness in this phase cannot be addressed by these methods. However, these calculations should provide a useful upper bound on the location of the actual MG-DL transition line.

The calculations of Ref. [27] applied to a model for BSCCO which considered only the *electromagnetic* interactions between pancake vortices moving on different layers, ignoring their (far weaker) Josephson couplings [89]. Such a model is *exact* for a layered system in the

limit of infinite anisotropy. For large but finite anisotropy, its predictions are quantitatively fairly accurate. It is argued here in some detail at the end of this section that the generic features of the results are relevant for the far more isotropic materials discussed in this paper.

The analysis of Ref. [27] was based on the replica method [83,54] applied to a system of point particles interacting via the Hamiltonian

$$H = H_{kinetic} + \frac{1}{2} \sum_{i \neq j} V(|\mathbf{r}_i - \mathbf{r}_j|) + \sum V_d(\mathbf{r}_i), \quad (4.1)$$

where $V(r)$ is a two-body interaction potential between the particles and $V_d(\mathbf{r})$ is a quenched, random, one-body potential, drawn from a Gaussian distribution of zero mean and short ranged correlations: $[V_d(\mathbf{r})V_d(\mathbf{r}')]=K(|\mathbf{r}-\mathbf{r}'|)$, with $[\dots]$ denoting an average over the disorder.

Using $[\ln Z] = \lim_{n \rightarrow 0}[(Z^n - 1)/n]$, one obtains, prior to taking the $n \rightarrow 0$ limit, a replicated and disorder averaged configurational partition function of the form

$$Z^R = \frac{1}{(N!)^n} \int \Pi d\mathbf{r}_i^\alpha \exp\left(-\frac{1}{2k_B T} \sum_{\alpha=1}^n \sum_{\beta=1}^n \sum_{i=1}^N \sum_{j=1}^N V^{\alpha\beta}(|\mathbf{r}_i^\alpha - \mathbf{r}_j^\beta|)\right). \quad (4.2)$$

Here α, β are replica indices and $V^{\alpha\beta}(|\mathbf{r}_i^\alpha - \mathbf{r}_j^\beta|) = V(|\mathbf{r}_i^\alpha - \mathbf{r}_j^\beta|)\delta_{\alpha\beta} - \beta K(|\mathbf{r}_i^\alpha - \mathbf{r}_j^\beta|)$ [27].

Eq. (4.2) resembles the partition function of a system of n “species” of particles, each labeled by an appropriate replica index and interacting via a two-body interaction which depends both on particle coordinates $(\mathbf{r}_i, \mathbf{r}_j)$ and replica indices (α, β) . This system of n species of particles can be treated in liquid state theory by considering it to be a n -component mixture [90] and taking the $n \rightarrow 0$ limit in the Ornstein-Zernike equations governing the properties of the mixture. These equations involve the pair correlation functions $h^{\alpha\beta}$ and the direct correlation functions $C^{\alpha\beta}$ of the replicated system. Assuming replica symmetry $C^{\alpha\beta} = C^{(1)}\delta_{\alpha\beta} + C^{(2)}(1 - \delta_{\alpha\beta})$ and $h^{\alpha\beta} = h^{(1)}\delta_{\alpha\beta} + h^{(2)}(1 - \delta_{\alpha\beta})$.

Ref. [27], obtained $h^{(1)}(\rho, nd)$ and $h^{(2)}(\rho, nd)$ for the layered vortex system in BSCCO using the HNC closure approximation. To estimate the inter-replica interaction $\beta K(\rho, nd)$, the principal source of disorder was assumed to be atomic scale pinning centers such as

oxygen defects [85]. (Similar point defects are believed to act as the principal sources of disorder in the systems discussed in this paper.) A model calculation then yields

$$\beta V^{(2)}(\rho, nd) = -\beta K(\rho, nd) \simeq -\Gamma' \exp(-\rho^2/\xi^2) \delta_{n,0}; \quad (4.3)$$

where $\beta V^{(2)}(\rho, nd) = \beta V^{\alpha\beta}(\rho, nd)$ with $\alpha \neq \beta$. $\xi \simeq 15\text{\AA}$ is the coherence length in the *ab* plane, and $\Gamma' \approx 10^{-5}\Gamma^2$ for point pinning of strength $dr_0^2 H_c^2/8\pi$, with d the interlayer spacing ($\sim 15\text{\AA}$), $\Gamma = \beta d \Phi_0^2 / 4\pi \lambda^2$ and $\beta = 1/k_B T$. Defect densities of the order of $10^{20}/\text{cm}^3$ are assumed in the calculation of the prefactor [27].

The calculated correlation functions $C^{(1)}(r)$ and $C^{(2)}(r)$ are then used as input into an appropriately generalized (replicated) version [27] of the density functional theory [91,19], in order to examine the effects of disorder on the freezing transition. Applying the replica treatment leads to the following functional in the $n \rightarrow 0$ limit:

$$\begin{aligned} \frac{\Delta\Omega}{k_B T} = & \int d\mathbf{r} \left[\rho(\mathbf{r}) \ln \frac{\rho(\mathbf{r})}{\rho_\ell} - \delta\rho(\mathbf{r}) \right] \\ & - \frac{1}{2} \int d\mathbf{r} \int d\mathbf{r}' [C^{(1)}(|\mathbf{r} - \mathbf{r}'|) - C^{(2)}(|\mathbf{r} - \mathbf{r}'|)] [\rho(\mathbf{r}) - \rho_\ell] [\rho(\mathbf{r}') - \rho_\ell] + \dots \end{aligned} \quad (4.4)$$

It is assumed that the density field is the same in all the replicas ($\rho^\alpha(\mathbf{r}) = \rho(\mathbf{r})$ for all α). The uniform liquid density is ρ_ℓ . This density functional resembles the density functional of a *pure* system with an *effective* direct correlation function given by

$$C^{eff}(|\mathbf{r} - \mathbf{r}'|) = C^{(1)}(|\mathbf{r} - \mathbf{r}'|) - C^{(2)}(|\mathbf{r} - \mathbf{r}'|), \quad (4.5)$$

In mean-field theory, the freezing transition of the pure system occurs when the density functional supports periodic solutions

$$\rho(\mathbf{r}) = \sum_{\mathbf{G}} \rho_{\mathbf{G}} \exp(i\mathbf{G} \cdot \mathbf{r}), \quad (4.6)$$

with a free energy lower than that of the uniform fluid [91,19]. Here \mathbf{G} indexes the reciprocal lattice vectors of the crystal and $\rho_{\mathbf{G}}$ represent the order parameters of the crystalline state. The properties of the freezing transition are controlled by $C^{eff}(q)$, the Fourier transform of $C^{eff}(r)$. In a one-order parameter approximation, only $C^{eff}(q)$ evaluated at the wave-vector

q corresponding to the nearest neighbour spacing a *i.e.* at $q = q_m = 2\pi/a$ is required as input. The one-parameter density functional calculation of Ref. [27] indicated that melting occurred when the $\rho_\ell C^{eff}(q = q_m)$ attained a value of about 0.8 [19]. This result agrees with the phenomenological Hansen-Verlet criterion for the freezing of a simple two-dimensional liquid [90]: Freezing occurs when the structure factor

$$S(q) = 1/(1 - \rho C^{eff}(q)), \quad (4.7)$$

evaluated at q_m *i.e.* $S(q_m)$ attains a value of about 5.

The following feature of the replicated density functional provides useful physical insight: Since $C^{(2)}(q_m) \geq 0$, and $C^{(1)}(q_m)$ is always reduced (although weakly) in the presence of disorder, the equilibrium melting line is always *suppressed* by quenched disorder. The analysis of Ref. [27] showed that this suppression was very weak at low H but systematically increased at large H , indicating the increased importance of disorder at high fields.

The semi-analytic approach to the suppression of the MG-DL phase boundary outlined here uses the following ideas:

1. The *diagonal* direct correlation function $C^{(1)}(q)$ is very weakly affected by disorder and can thus be approximated by its value in the absence of disorder.
2. The off-diagonal direct correlation function $C^{(2)}(q)$ is a strong function of disorder and of H , the magnetic field
3. $C^{(2)}(q)$ is well approximated at $q = q_m = 2\pi/a$ by its value at $q = 0$.

Since the Hansen-Verlet condition is satisfied along the melting line, the following is true at melting:

$$\rho_\ell C^{eff} = \rho_\ell(C^{(1)}(q_m) + C^{(2)}(q_m)) \simeq 0.8. \quad (4.8)$$

Now $C^{(2)}$ is a sharply decaying function in real space; its support is ξ^2 , which for typical $H \ll H_{c2}$, is far less than a^2 . In Fourier space, therefore, its value at $q = q_m$ is close to its value at $q = 0$. We can approximate [90,4]

$$C^{(2)}(r) \simeq -\beta V^{(2)}(r). \quad (4.9)$$

This scales with temperature as Γ^2 , implying that

$$\rho_\ell C^{(2)}(q_m) \sim \frac{B}{T^2}. \quad (4.10)$$

Note that $C^{(2)}(q_m)$ increases as B is increased or as T is decreased, as is intuitively reasonable.

We turn now to $C^{(1)}(q_m)$. $C^{(1)}(q_m)$ increases with a decrease in T ; reducing T increases correlations. The variation in $C^{(1)}$ is expected to be smooth. We can therefore write

$$C^{(1)}(q_m; T - \Delta T, B) = C^{(1)}(q_m; T, B) - q(B, T)\Delta T, \quad (4.11)$$

where $q(B, T)$ ($q < 0$) is a smooth function of B and T close to the melting line. We are trying to find the effects to first order of adding $C^{(2)}$, so (B, T) can be replaced by (B_m, T_m) in Eq. 4.8 above and $C^{(1)}(q_m; B_m, T_m)$ by its value at freezing for the pure system: $C^{(1)}(q_m; B_m, T_m) \simeq 0.8$. The further approximation of neglecting the B and T dependence of q *i.e.* $q(B_m, T_m) \simeq q$, with q a constant can also be made; at melting this dependence should be small provided $a \ll \lambda$.

An approximate expression for the suppression of the melting line from its value $(B_m, T_m) = (B_m(T), T)$ can now be obtained. Using $q\Delta T_m = pB_m/T_m^2$,

$$\Delta T_m = \frac{pB_m}{qT_m^2} = m \frac{B_m}{T_m^2} = m \frac{B_m(T)}{T^2}, \quad (4.12)$$

with $m = p/q$ approximately constant. Here ΔT_m is the shift in the melting temperature induced by the disorder. This relation predicts a larger suppression of the melting line at higher fields and lower temperatures, precisely as in the work of Ref. [27] and in the experimental data. Given a parametrization of the pure melting line, Eq.(4.12) can be used to estimate the effects of weak disorder on this line.

This result can be combined with results from a calculation of the melting line in the pure system to obtain a simple analytic formula for the MG-DL phase boundary. At low fields, a Lindemann parameter-based calculation of this phase boundary yields

$$B_m(T) = C(T - T_c)^2, \quad (4.13)$$

where T_c is the critical temperature and C is a constant [1]. Coupled with Eq.(4.12) above, this yields, in the presence of disorder

$$B_m^{dis}(T) = C(T + \frac{Cm(T - T_c)^2}{T^2} - T_c)^2. \quad (4.14)$$

This relation is plotted in Fig. 5 for different values of m together with the melting line in the absence of disorder *i.e.* with $m = 0$. The data shown in Fig. 5 use a T_c value of 7K, as appropriate for 2H-NbSe₂, a prefactor C of 1.15 kG (chosen purely for illustrative purposes) and values of $Cm = 0, 0.2$ and 0.5 . Note that the suppression of the pure melting line by disorder is very weak if m is small. This suppression becomes progressively large as m is increased, or alternatively, at a lower temperature (larger H) for given m . These results are consistent, both qualitatively and quantitatively with the numerical results of Ref. [27]. They are also consistent with the experimental results of Ref. [34] which find that fits of the T_p line in disordered samples of 2H-NbSe₂ to a Lindemann-type expression are accurate at low field values but become increasingly inaccurate at larger fields. At large H the T_p line is systematically suppressed to lower T *vis a vis.* the fit, this suppression becoming apparent at lower fields for more disordered samples.

These results were motivated using a parametrization of vortex lines in terms of interacting pancake vortices, a description valid for highly anisotropic layered superconductors in which the c-axis coherence length is far smaller than the interlayer spacing. How do they generalize to interacting *lines*? The calculation itself uses two quantities – the direct correlation function in the fluid phase for the pure system, evaluated at a wave-vector equal in magnitude to the first reciprocal lattice vector of the crystal G_1 *i.e.* $C(|k_{\perp}| = |G_1|, k_z = 0)$. This quantity accounts for the tendency towards ordering at the length-scale of the inter-vortex spacing. The calculation which lead to Eq.(4.12) above used only two properties of this correlation function: (i) the pure system freezes when the correlation function evaluated at this wave-vector achieves a particular (universal) value and (ii) the variation of this quantity upon a reduction of temperature can be parametrized simply, essentially linearly.

Both these features should apply to the case of interacting lines. Numerical simulations of interacting lines provide some evidence for similar quasi-universal attributes of the melting transition as seen in two and three dimensions, both in simulations and in experiments [19].

The other quantity required in the calculation, $C^{(2)}$, derives from properties of the correlation function of the disorder potential $K(x - x')$. This is independent of the (line or point) nature of the model for the flux-line system used. Thus, it is apparent that the result obtained in Eqn.(4.14), should be a fairly robust one which does not depend in detail on the fact that it was derived using results obtained from a model of interacting pancake vortices with only electromagnetic interactions.

V. COMPARISON TO EXPERIMENTAL RESULTS

Section III obtained expressions for the $B - T$ phase boundary separating BG and MG phases given $H_{c2}(T)$ and $\lambda(T)$. In Section IV, qualitative and quantitative arguments were provided for the effects of weak disorder on the MG-DL transition line. This section compares the predictions of these sections with some of the available data on the phase boundaries in the experimental systems studied in Ref. [35] as well as data on the high- T_c material $\text{Nd}_{2-x}\text{Ce}_x\text{CuO}_y$ (NCCO).

We do not attempt fits either to the YBCO or BSCCO data (although experiments relating to these are discussed in some detail in the following section), primarily because the results derived above ignore the effects of thermal renormalization of disorder, which are not negligible in these materials. (Effectively, these should lead to a strong T dependence of Σ , which cannot be treated as a constant.) We have also not attempted to provide highly accurate fits to the experimental data in any of the cases below, since we merely wish to demonstrate that reasonable agreement with data can be obtained within the theoretical framework described in this paper.

- **2H-NbSe₂:** Fig. 6 plots the experimental data for (H_{pl}, t_{pl}) in single crystals of 2H-NbSe₂, taken from Fig. 2(a) of Ref. [34] together with a best fit line based on

Eqn.(3.14). As argued here (also see Ref. [34]), this line represents the BG-MG phase boundary; t_{pl} is T_{pl}/T_c .) An upper critical field of $H_{c2}(0) = 46\text{kG}$ is assumed in the normalization of b . Assuming $\kappa \sim 16$, $p \sim 1$ and $c_L \sim 0.22$, yields $\Sigma \sim 60.0$. The data are represented by an almost straight line over this field range, with deviations to the tune of about 1kG appearing in the lower temperature range spanned by the data. The linear behaviour of $B_{c2}(T)$ assumed in the use of Eq.(3.14), is a feature of the experimental data in this field and temperature range.

- **CeRu₂:** Data points representing the BG-MG phase boundary, extracted from plots of (H_{pl}, T_{pl}) , in Fig. 3(b) of Ref. [31] are shown in Fig. 7, together with a best fit based on Eqn.(3.17). An upper critical field of 68kG and a T_c of 6.2 K is assumed in the normalization to aid comparison to experimental data. Values of $c_L \sim 0.18$, $\kappa \sim 1$ and $p \sim 1$ are assumed, yielding $\Sigma \sim 0.01$.
- **Ca₃Rh₄Sn₁₃:** Points extracted from the plots of (H_{pl}, t_{pl}) in Fig. 3(c) of Ref. [34] are shown in Fig. 8, together with best fits based on Eqn.(3.17). An upper critical field H_{c2} of 45 kG is assumed in the normalization of the y -axis in the comparison to experimental data. Values of $c_L \sim 0.18$, $\kappa \sim 1$ and $p \sim 1$ are assumed, yielding $\Sigma \sim 0.01$.
- **NCCO:** Fig. 1 of Ref. [118] illustrates a very successful phenomenological fit to the experimental data on the BG-MG phase boundary in NCCO. This phase boundary was assigned to the locus of onset points of the fishtail anomaly. We plot the line obtained using Eq.3.17 with $\Sigma = 0.001$, multiplied by an appropriate prefactor chosen to allow both curves to overlap as far as possible together with this fitting form $B_m = B_0(1 - (T/T_c)^4)^{3/2}$ in Fig. 9. (The somewhat smaller value of Σ here should reflect the increased role of disorder in these systems, as reflected in the parameter p .) Eq.3.17 predicts a marginally smoother and slower variation of the transition curve than the fitted form, but the qualitative trends appear to be the same. As a cautionary note,

the identification of the BG-MG phase boundary with the onset curves of the fishtail effect is not universally accepted.

VI. DISCUSSION OF EXPERIMENTS

To what extent are either of the two scenarios outlined in the Introduction supported by the experiments and the simulations? To support our proposal of the second scenario as a *generic* one for disordered type-II superconductors, we take the following approach: First, we will show that the situation in which a sliver of intermediate phase intervenes between the BG and the DL phases is actually far more common than earlier realized. We do this by showing that more recent experimental data on the high- T_c materials which initially showed a single melting transition strongly favours a two-step transition. Second, we will show that the first of the two transitions out of the BG phase illustrated in Fig. 2, the “fracturing transition” into the MG phase, may not show up at all in many types of experiments commonly used to probe phase behaviour, such as measurements of the dc magnetization.

This second point is illustrated through the following estimate: If a finite density of unbound dislocations ρ_d enters the sample at the BG-MG phase boundary, the magnetization discontinuity across this boundary should scale, for small $\rho_d \sim 1/R_d^2$, as

$$\Delta M \sim \Delta M_0 (a/R_a)^2, \quad (6.1)$$

where ΔM_0 is the magnetization jump in the pure system at the melting transition. Even if $R_a/a \sim 30$, the corresponding induction jump $\Delta B \sim \Delta M$ is of order $10^{-3} M_0$ or within noise levels in a typical experiment [15,46].

Some of the discussion will focus on the peak effect in critical currents seen close to the H_{c2} phase boundary in weakly disordered systems. Within a simple Bean model [92] for the critical state, the real part of the complex susceptibility, χ' , obeys

$$\chi' \sim -\beta \frac{j_c}{h_{ac}}, \quad (6.2)$$

once the ac field has penetrated fully within the sample. Here β is a geometrical quantity related to the shape of the sample and h_{ac} is the amplitude of the ac field. Thus, increases in the critical current density j_c translate to reductions in χ' . Transport measurements access j_c more directly, although the presence of Joule heating in the transport measurements is often a significant factor, particularly in the peak regime where thermal instabilities are strong.

The observation of an anomaly in magnetic hysteresis in the high- T_c superconducting oxides has attracted much attention in the past decade. This anomaly, an *increase* in the width of the magnetization hysteresis curve with field and a concomitant increase in j_c (following an initial increase and subsequent decrease due to complete field penetration, the “first peak”) is the “second peak” or “fishtail” anomaly [93–95]. The relation between j_c and the width of the hysteresis loop follows from:

$$j_c \propto \Delta M = M(H \uparrow) - M(H \downarrow), \quad (6.3)$$

the difference in values of the magnetization on the increasing and decreasing branches of the hysteresis loop. While several explanations have been proposed for this phenomenon, this behaviour is now believed to be correlated, at least approximately, with the field-driven transition between two vortex solid phases, identified by a large body of work as BG and MG phases [97].

As pointed out in Ref. [35], the very structure of the phase diagram of Fig. 2 mandates the following: The peak effect in T scans at intermediate values of H should evolve smoothly and continuously into behaviour characteristic of the BG-MG field driven transition, both at low and high H . This is a simple consequence of the absence of a multicritical point. Insofar as the fishtail effect indicates a field-driven transition from a BG phase to the MG phase, signatures of the fishtail phenomena should connect smoothly to signals of the peak effect on T scans. Thus, it is natural to argue for a connection between fishtail effects (in H scans) and peak effects (in susceptibility and transport measurements on T scans); both are phenomena which refer to the *same* underlying phase transition out of the Bragg glass

phase.

What is less clear is the precise connection of the fishtail feature to the underlying transition. There are at least three distinct characteristic fields associated with the fishtail feature. These are the onset field H_o (also called H_{min}), the “kink” field H_k (also called H_3), the field value at which the magnetization shows a kink, and the peak field H_p [98] (also called H_{sp}). The temperature dependences of these features can be quite different. For example, in YBCO, the onset is most often a monotonically decreasing function of T , while the kink and peak features can show non-monotonic behaviour. It has been argued that the kink feature most probably signals the underlying transition [98], although there does not appear to be universal agreement upon this point.

A. Low- T_c Systems

This subsection summarizes features of the data on three low- T_c materials: 2H-NbSe₂, CeRu₂ and Ca₃Rh₄Sn₁₃. Some aspects of this discussion have already appeared elsewhere [35], so the discussion here is brief.

1. 2H-NbSe₂

Banerjee *et. al.* have reported data on ac susceptibility measurements on single crystals of 2H-NbSe₂ of differing purity [32]. The purest crystal, X, has a T_c of 7.2K, while a crystal of intermediate purity, Y has a T_c value of about 7K. A more disordered crystal, Z, has a T_c value of about 6K. The relative purity of the crystal was inferred from the values of j_c/j_{dp} for these materials.

In sample X, T_p (where j_c first begins to increase) and T_{pl} (where j_c peaks) are almost coincident. The data indicate an extremely sharp peak, with a width comparable to or even smaller than the width of the superconducting phase transition in zero applied field [32,34]. The two-step nature of the transition is obvious in the sample with intermediate level of disorder, while this is a prominent feature of the most disordered crystal. The locus of T_p

and T_{pl} lines, as functions of H , almost coincide in X, are resolvable as separate lines in Y and are clearly visible as separate features in Z. In sample Z, the T_p and T_{pl} lines clearly move apart at higher field values, suggesting that their ultimate fate would be to expand into the broad regime of vortex glass expected at high field values [35].

In the most disordered samples of 2H-NbSe₂, onset and peak values of the peak effect are clearly and separately distinguishable down to low field values, where the T_p line begin to turn around, signalling the appearance of a reentrant glassy phase [51,34,35]. This feature suggests that the glass at high fields and the glass at low fields are *smoothly connected*, at least in samples with intermediate to high levels of disorder [35]. As Ref. [34] indicates, for purer samples, the extreme narrowness of the peak makes resolution of the features of the intermediate sliver region very difficult, although the peak itself is obtained to low field values.

Ravikumar and collaborators see a discontinuity in the dc magnetization across the peak regime in single crystals of 2H-NbSe₂ supporting the existence of a melting transition. The experiments could not resolve whether this feature was connected to T_p or to T_{pl} [99]. There is some evidence that the magnetization anomaly is connected to T_p from the combined magnetization and ac susceptibility measurements of Saalfrank *et. al.* [100]. These experiments see a sharp peak in the derivative dM/dT , most likely associated with a step in the magnetization as a function of T at the location of the T_p line. Saalfrank *et. al.* note that the main peak of dm/dH showed no reentrant behaviour while the peak in the ac susceptibility shifted to lower temperatures at very low applied field values, supporting the earlier proposal of a reentrant transition to a low field glassy phase [51]. As argued here, magnetization discontinuities signalling the transition to the liquid should generically be associated with the T_{pl} line.

A substantial body of work exists on anomalies associated with the peak effect regime, particularly in the case of 2H-NbSe₂ [31,32,36,33,68–70]. Ref. [35] proposed that these anomalies should be primarily associated with the *static* properties of the intervening vortex glass (equivalently, multi-domain) phase. This idea is discussed briefly here: (i) In the

experiments, the transition to the anomalous peak effect regime on temperature scans from within the BG phase occurs discontinuously via an apparent first-order phase transition. Thus the anomalies seen in the peak regime *cannot* be linked to the dynamics of plastic flow of a vortex lattice or even quasi-lattice state since the lattice phase is *not* linked smoothly to the intervening sliver phase (ii) the fact that peak-effect related anomalies in the depinning of a vortex lattice are *only* seen in the peak regime indicates strongly that a static phase transition may be involved and the solution cannot be traced to the dynamics alone. This point is stressed since many $T = 0$ simulations of plastic flow (which do not have a phase transition) appear to be able to reproduce (some but not all) features of the peak effect phenomenon [101]. Finally, (iii) the concept of “softening” of elastic constants leading to a peak effect and associated anomalies may well be irrelevant; there appear to be few strong pre-transitional effects at the fracturing transition and the peak effect signal in χ' jumps discontinuously in the experiments.

2. $\mathbf{Ca_3Rh_4Sn_{13}}$

The $\mathbf{Ca_3Rh_4Sn_{13}}$ system was first studied by Tomy *et.al.*, who drew attention both to the prominent peak effect seen in this system and the related compound $\mathbf{Yb_3Rh_4Sn_{13}}$ as well as to the substantial similarities obtained with peak effects in other superconducting systems, notably $\mathbf{UPd_2Al_3}$ and $\mathbf{CeRu_2}$ [39,40]. Tomy *et. al.* obtained H^* , the field at which the onset of the peak occurred both from susceptibility and dc magnetization experiments. Plots of H^* *vs.* T , show that the transition curve (which is interpreted here as signalling the BG-MG phase transition) appears to connect to the H_{c2} line only at $T \rightarrow T_c$. The region of fields and temperatures above H^* was found to show strongly irreversible behaviour, in contrast to the behaviour below H^* .

Sarkar *et. al.* have studied in some detail the magnetic phase diagram of this compound through ac susceptibility measurements [41]. Susceptibility data in this material also show the characteristic two-step feature exhibited by $\mathbf{2H-NbSe_2}$ at intermediate fields. At low fields,

the T_p and the T_{pl} lines come close but do not appear to merge at least until temperatures fairly close to T_c . The large field data are consistent with the bending backwards of the T_{pl} line indicating that the intermediate regime of vortex glass expands out at low temperatures and high fields, precisely as suggested in Fig. 2.

3. CeRu₂

Early work on single crystals of the cubic Laves phase (C15) intermetallic superconductor CeRu₂ by Huxley *et. al.* [109,38] described a sharp reversible to irreversible transition in the mixed state close to H_{c2} [103]. The possible relation of these results to a phase transition into a novel modulated superconducting phase (the FFLO state [110]) was discussed by these authors and later investigated extensively by others. Careful longitudinal and Hall resistivity measurements by Sato *et. al.* have revealed that the peak effect survives in this material to far larger fields than the original measurements indicated [112]. Fig. 2 of Sato *et. al.* summarizes the results of their measurements and is to be compared to Fig. 2 of this paper; the $H_p(T)$ curve in this figure is to be related to our $T_{pl}(H)$. Note that this line appears to extrapolate smoothly to T_c , although signatures of magnetic hysteresis are not observed below about 2T. Sato *et. al.* point out that their observations rule out the FFLO state as a possible explanation of the PE anomaly. These experiments suggest that pinning is substantially *weakened* at intermediate H , although signatures of a peak effect remain.

Transport measurements on CeRu₂ by Dilley *et. al.* show a striking peak effect signal, together with a strong dependence of measured quantities on the magnitude of the transport current [113]. Dilley *et. al.* note the existence of strong thermal instabilities in the intermediate peak effect regime, together with profound hysteresis. Many of these features are seen in 2H-NbSe₂ [49]. Muon-spin rotation studies of CeRu₂ [114] have been invoked to suggest that a FFLO mechanism may be involved in this material. These measurements see a rapid decrease in the second moment $\langle \Delta B^2 \rangle$ of the field distribution function across a line in the phase diagram; such a decrease naively suggests a sharp increase in the penetration

depth λ . Yamashita *et. al.* point out that pinning induced line distortions should generically lead to broadening of the line-width and not to its reduction. However, a sharp transition to a multi-domain phase, with *short-ranged correlations in the field direction* would give essentially similar results to those of Yamashita *et. al.* [21].

In a recent illuminating study of the peak effect anomaly in single crystals of CeRu₂, Tenya *et. al.* have shown that the peak effect lies in the *irreversible* region of the phase diagram, counter to some previous work [102]. Their results establish the following: The onset of the peak, at T_{pl} , corresponds to an abrupt transition from a defective lattice to a regular one. The state of the sample in the peak regime is argued to be intermediate between an ordered structure and a fully amorphous one. These ideas are closely related to those presented here.

Work by Banerjee *et. al.* shows a remarkable similarity between the vortex phase diagram in a weakly pinned single crystal of CeRu₂ with that of more disordered samples of 2H-NbSe₂ [33,34]. This close similarity has been used to argue that the origin of peak effect anomalies in these two materials may well be common [33,34].

B. High-T_c Systems

This subsection summarizes data relating to peak and fishtail effects in four high-T_c materials: BSCCO, YBCO, NCCO and (K,Ba)BiO₃.

1. YBCO

Early torsional oscillator experiments of d'Anna *et. al.* measured complex response in the PE regime of untwinned YBCO [115]. A prescient comment of d'Anna *et. al.* regarding their data is particularly noteworthy, for its overlap with the proposals made here. d'Anna *et. al.* commented that *..the melting phenomenon, giving rise to the peak effect, the loss peak and the kink in resistivity in so-called clean YBCO, is in fact a complex, two-stage phenomenon..* [115]. The first stage was ascribed to a lattice *softening* leading to a change

in the pinning regime, as in conventional approaches to the peak effect, while the second was associated with a collapse of the shear modulus at melting and/or a decoupling transition.

In transport measurements in fields upto 10T, d'Anna *et. al.* found two boundaries, between which noise due to vortex motion rose to a maximum [108]. The lower boundary was identified with the peak effect; the noise falls below the limit of resolution at another boundary, somewhat above the first one. These results are to be compared to those obtained in similiar transport [36] and susceptibility [33] measurements on 2H-NbSe₂, which see a sharp increase in noise amplitudes only in the peak effect regime, with a discontinuous onset.

Ishida *et. al.* have simultaneously measured ac susceptibility and magnetization and see a sharp peak effect in the field range 0.1- 1.5T [116]. The peak of the peak effect signal in ac susceptibility was found to correlate exactly to the location of the magnetization jump which signals melting. Ishida *et. al.* draw attention to a small dip feature in χ' at a temperature T_s , preceding the peak and the associated magnetization discontinuity. This subtle feature is attributed to a “synchronization effect between lattice and pinning sites”, as a consequence of lattice softening. (The possibility of such synchronization has often been discussed in the past as a mechanism for the peak effect [59].) The close similarity of this phenomenology with that discussed for low- T_c systems in Ref. [35] is emphasized here. Ishida *et. al.* also comment on the enlarged regime in which χ' shows non-trivial signatures of the transition in comparison to the magnetization jump which occurs at a sharply defined temperature.

These results are very simply understood using Fig. 2. We would argue here for the natural identification $T_s = T_{pl}$. The width of the transition region is related to the width of the sliver phase, argued here to be always finite in scenario (2), while the most prominent signatures of melting should generically be obtained across a *line*, the MG-DL transition line, which we suggest is the true remnant of the vortex lattice melting line in the pure system.

Shi *et. al.* have observed a “giant” peak effect in ultrapure crystals of YBCO [117] at fields ranging from 0-4T [117]. This feature is most prominent at intermediate H , repro-

ducing the phenomenology of the peak effect in 2H-NbSe₂. Shi *et. al.* demonstrate that the jump in the magnetization coincides, to within experimental accuracy, with T_p . Shi *et. al.* also comment that peak effect signals can be seen in fields up to 6T, although only by going to far higher ac drive frequencies (1 MHz). This is consistent both with the weakening of the effective disorder in the intermediate field regime and the existence of a sliver phase with finite width.

Rydh, Andersson and Rapp [122], in transport studies of untwinned YBCO, obtain three regimes of flow: (1) a low temperature creep regime (2) an intermediate flow/ creep regime (3) a small regime in which the resistivity drops as a consequence of the peak effect and (4) a high-temperature fluid regime. Rydh *et. al.* find that the dip in resistivity is correlated to the melting transition. It is suggested that the width of region III reflects a distribution of melting temperatures in the solid and argue that the onset of melting occurs at the minimum of the resistive dip. In our interpretation, regime III would be assigned to the multi-domain regime.

Suggestive work by Rassau *et. al.* [79] studies magnetization relaxation in the vortex solid phase of YBCO. Rassau *et. al.* argue that a well-defined region exists below T_m which can be quantified as a coexistence of solid and liquid phases and demonstrate that the vortex solid state can be pinned with different strengths, depending on prior history. The processes which lead to these different states arise across a narrow temperature region immediately below T_m . This is precisely the phenomenology indicated by experiments on 2H-NbSe₂ and related low- T_c compounds which show a peak effect; we draw the readers attention to Ref. [72] in this regard. We would argue that the intermediate region interpreted by Rassau *et. al.* as relating to a regime of two-phase coexistence is our multidomain phase.

Detailed insights into the vortex phase diagram of untwinned YBCO comes from the work of Nishizaki *et. al.*, who present magnetic measurements on the vortex lattice in a clean sample [77]. At large H and low T , the data show a fishtail feature in the magnetization which narrows, as T is increased, to a bubble-like feature. Nishizaki *et. al.* discuss the existence of an *anomalous reentrant* behaviour in j_c , inferred from their data via a Bean

model-based calculation, for temperatures in the range $68K < T < 74K$. They find that j_c drops very sharply at low fields to almost unobservable levels, then picks up to form a peak; while hysteresis decreases and disappears at $T = 70K$ in the intermediate field region ($3.5K \leq \mu_0 H \leq 6T$), it reappears again and is maximum around $10.5T$.

Nishizaki *et. al.* comment that this reentrant magnetization is seen only in high quality samples with a lower pinning force and comment that these results indicate that the pinning force for the untwinned samples is remarkably reduced in the intermediate-field regime. This comment accords with our earlier discussion of the strong effects of thermal renormalization of disorder in the intermediate field, interaction dominated regime. The *shape* of the irreversibility line in the data of Nishizaki *et. al.* is particularly noteworthy in this respect.

Very accurate ac susceptibility measurements using a local Hall probe have been performed by Billon *et. al.* [87] in the field and temperature regimes in which Nishizaki *et. al.* find reversible behaviour and a single melting transition. These experiments find that the critical current is actually finite below the melting temperature but is extremely small ($\sim 0.4A/cm^2$), leading to an irreversible magnetization unresolvable by standard superconducting quantum interference device magnetometry. These experiments see a peak effect *below* the apparent melting transition, a feature *inaccessible* in conventional SQUID based measurements. These results clearly illustrate that signals of a two-step transition in weakly disordered single crystals of high- T_c materials may be very hard to access, particularly if discontinuities in j_c or magnetization across the first transition are small.

Nishizaki *et. al.* argue that in the high temperature region above T_{cp} , the BG-MG transition line ($H^*(T)$ in the notation of Nishizaki *et. al.*) *turns down* and meets the $H_m(T)$ melting line *below* H_{cp} for irradiated YBCO. Thus they argue that the second peak effect just below T_m may be closely related to enhanced vortex pinning due to vortex lattice softening *i.e.* the conventional peak effect. The connection of this observation to the discussion of the phenomenology of the peak effect presented in Ref. [35] is stressed here, as is the link outlined earlier between fishtail features and PE features, given the phase diagram of Fig. 2.

Nishizaki and collaborators have also reported results on the phase diagram of untwinned YBCO crystals on varying the Oxygen stoichiometry. For fully oxidized YBCO crystals ($\text{YBa}_2\text{Cu}_3\text{O}_y$, $y \simeq 7$, $T_c \simeq 87.5\text{K}$), Nishizaki *et. al.* find that the first order melting transition can be tracked to high fields (upto 30T). For optimally doped YBCO ($\text{YBa}_2\text{Cu}_3\text{O}_y$, $y \simeq 6.92$, $T_c \simeq 93\text{K}$) and slightly underdoped YBCO, it is suggested that a vortex slush phase can exist between the second-order and first-order transition lines. This “slush” phase intervenes between the glass and the liquid phases of the vortex system [76].

How is the slush phase to be understood using the ideas presented here? Fig. 2 presents a particularly simple topology for that part of the phase diagram which involves the MG-DL transition line, in which the first-order MG-DL transition becomes continuous for sufficiently large H . Such a phase diagram does not contain a slush phase. However, the situation could be more complex. For example, the continuous part of the MG-DL transition line obtained at large H could meet the first-order part at a critical end point (CEP). The first-order transition above the CEP would then be interpreted as a liquid-liquid transition, between phases of different densities, with a further, *symmetry-breaking* transition into a glassy phase occurring at lower T . The phase with a larger average density would then represent the “slush” phase [104].

An paper by Abulafia *et. al.* [105] studies magnetization relaxation in YBCO crystals, finding two distinct regimes of relaxation below and above the peak in the fishtail magnetization. These regimes were interpreted by these authors as signalling plastic vortex creep in the vortex lattice state. This interpretation has been questioned by Klein *et. al.* [106] (see also Ref. [107]) who argue that the fishtail effect marks a transition from a low-field ordered phase to a high-field glassy structure, an interpretation in agreement with ours. It is argued that *topological order (in the glassy phase) can be quenched at large length scales, with diverging barriers as j goes to zero* [106], an idea in agreement with our suggestion that the multi-domain glass has *fixed* topological order unlike the liquid, but glassy attributes. With this interpretation of the data of Abulafia *et. al.* their phase diagram (Fig. 4 of Ref. [105]), is very similar to the one we have proposed. In particular, the melting line and the

glass transition line (if it is identified with the locus of fishtail peak positions), converge only at $T \rightarrow T_c$.

Recent experiments by Pissas *et. al.* [121] on single crystal YBCO samples probe somewhat more disordered samples than those studied by Nishizaki *et. al.*. An abrupt change in slope of the increasing part of the virgin magnetization curves is seen. This feature is sharpest at intermediate T ; it broadens or vanishes at low T and is hard to discern for $T > 75K$. This abrupt change of slope, associated with a curve $H_3(T)$, merges with the second peak feature $H_{sp}(T)$ at a temperature T^* . Both the irreversibility line and the melting line lie *above* the second peak line. The structure of this phase diagram is to be compared to the ones shown in Ref. [35] for low- T_c materials in which the irreversibility line lies above the BG-MG transition line. The phase behaviour depicted in Fig. 4 of Pissas *et. al.* agrees well with the ideas presented here as well as the structure of Fig. 2 with the identification of H_3 as the BG-MG transition line.

To summarize, experiments on untwinned YBCO support the presence of an intermediate phase which intervenes in equilibrium between BG and DL phases, particularly at low fields ($H < 2 - 4T$). For larger H , a substantially reversible regime is entered, close to the putative melting transition. In this regime, precision experiments see weak residual irreversibility as well as a peak effect just below the melting transition. (SQUID-based magnetization experiments see only a single transition here.) It is natural to interpret these features as signalling the continuation of the sliver between high and low-field ends as well as the profound weakening of disorder effects in the intermediate H , interaction dominated regime, as a consequence of the averaging of disorder by thermal fluctuations. We argue that this weakening of effective disorder is responsible for the *apparent* single-step transition experiments see at intermediate H . At still higher fields, the fishtail feature splits off from the melting line, yielding an expanding regime of vortex glass phase. The magnetization discontinuities associated with this melting line survive to very high fields ($\sim 30T$) in the purest samples. For more disordered samples, the separation between the BG-MG and the MG-DL transition lines is plainly apparent.

2. BSCCO

The earliest data to provide thermodynamic evidence of a sharp melting transition in single crystals of a high- T_c superconductor were the Hall probe measurements of Zeldov and collaborators on BSCCO [15]. These experiments obtained a discontinuity in the magnetic induction sensed by Hall probes at the surface of a BSCCO platelet. Practically no hysteresis was seen at any one probe, while different probes showed slightly different values for the melting field, indicating a spread of melting temperatures within the sample. The temperature driven melting transition in relatively pure single crystals of BSCCO occurs in a highly reversible regime. As reported for YBCO, the irreversibility line actually lies *within* the domain of the solid phase for clean crystals. These experiments see a single melting transition for weakly disordered systems. These and related experiments supported earlier structural evidence, from neutron scattering [14] and muon-spin rotation [75] for a sharp transition out of a quasi-lattice phase on increasing both B and T .

Very recent magneto-optic measurements by Soibel *et. al.* have reexamined this issue [46]. These experiments see a global rounding of the transition as a consequence of quenched disorder, argued by these authors to be due to a *broad distribution of local melting temperatures at scales down to the mesoscopic scale* [46]. These experiments reveal a remarkable and complex coexistence of fluid and solid domains in the larger crystals with the properties that while the local transition is sharp, the global solid-liquid transition is rounded by quenched disorder. Soibel *et. al.* found that the interfacial tension between solid and fluid phases was very small, indicating that the vortex melting process was governed to a large extent by disorder.

Recent muon-spin rotation experiments, on three sets of crystals whose properties range from overdoped to underdoped, show very clear indications of a two step transition, as pointed out by the authors. The first transition on increasing T was associated with a decoupling transition between the layers. In contrast, in our picture, this would be the transition into a multi-domain phase. This identification is supported by the observation of

α values close to unity in this phase indicating a substantial degree of local order.

Soibel *et. al.* see substantial “supercooling” across the first-order melting transition, with relatively small domains of fluid coexisting with domains of solid. The putative supercooled state then transforms abruptly into the crystal. We point out here that precisely such a scenario would be obtained in the context of the phase diagram of Fig. 2 with the single proviso that the intermediate “coexistence” regime which Soibel *et. al.* see would be assigned to our proposed “multidomain” state, an *equilibrium* phase with glassy properties. This is entirely consistent with our interpretation of the muon-spin rotation results of Blasius *et. al.*. We point out that from related studies on 2H-NbSe₂, it is known that the intermediate state on field cooling is relatively highly disordered, with short-ranged correlations resembling those in the liquid. By analogy, one would expect similar disordered states to be seen in the BSCCO case on field cooling, precisely as seen [46].

Ooi *et. al.* in a study of vortex avalanches in BSCCO through local magnetization and local permeability measurements, see a stepwise expulsion of vortices in a distinct temperature regime *below* the first-order transition on decreasing temperature scans [48]. This expulsion ceases abruptly below a second, lower temperature called by these authors as T_d. In between T_M and T_d, the experiments see broad-band noise with a power law spectrum. This phenomenology precisely reproduces related noise data in the peak effect regime of 2H-NbSe₂ and related systems.

Ooi *et. al.* also report a possible single step transition for weakly disordered samples and a *temperature-dependent* peak effect, which they associate with inhomogeneities in the melting field, for more disordered samples [124]. These results, presented as schematics as Fig. 5 of Ooi *et. al.* have interesting parallels with the phase diagrams presented here. We would argue that the regime that Ooi *et. al.* assign to inhomogeneities in the melting field should be attributed instead to a genuine thermodynamic phase, the sliver of disordered MG phase, which intervenes between the BG and DL phases.

A simulation by Sugano *et. al.* finds clear evidence for a two-stage melting of the disordered vortex-line lattice in BSCCO [125]. These authors find that the low-field melting

transition out of the Bragg glass occurs always via an intermediate “soft” glass phase; their phase diagram (Fig. 3 of Ref. [125]) is to be compared to the one shown in Fig. 2. Their proposal that the glassy phase is subdivided into strongly pinned and weakly pinned regimes has interesting overlaps with our suggestion of the increased importance of non-equilibrium effects at low T .

3. NCCO

The onset of the fishtail peak in magnetization measurements on a $\text{Nd}_{1.85}\text{Ce}_{0.15}\text{CuO}_{4-\delta}$ crystal, a layered cuprate system with substantial anisotropy and a relatively low T_c (~ 23 K) has been probed via local magnetization measurements using an array of Hall probes [118]. These experiments (in particular the phase diagram of Fig. 1 of Ref. [118]), show an onset field for the peak effect H_o which is always distinct from the irreversibility line separating an “entangled solid” phase from the vortex liquid phase. This phase diagram supports the ideas presented here, in particular the contention that a single sharp melting transition out of the BG phase is *not* generic (as scenario (1) would suggest) and provides strong support for scenario (2).

4. (K,Ba)BiO₃

Small angle neutron scattering studies of the isotropic high- T_c material (K,Ba)BiO₃ ($T_c \sim 30K$) suggest a phase diagram which is very close to the one displayed in Fig. 2 of this paper [123]. In this system, as in the NCCO system discussed previously, the transition line between the quasilattice and the glassy state always lies *below* the transition line separating the glass from the liquid. Klein and collaborators comment that the SANS data in this system support the connection of the fishtail effect with the transition to a glass out of the quasi-lattice BG phase [123]. In addition, another interesting feature of the data is the relatively smooth decrease in the intensity of a Bragg peak on field scans, while the

width of the peak remains virtually constant, suggesting a relatively high degree of local correlations in the putative vortex glass phase, as we would expect for a multi-domain solid.

VII. CONCLUSIONS

This paper has presented arguments in favour of a generic phase diagram for weakly disordered type-II superconductors. This phase diagram, Fig. 2, differs from others proposed earlier. We suggest that the relatively ordered BG phase *generically* transforms into an intermediate glassy state with solid-like correlations out to relatively large length scales rather than directly into a liquid. We have pointed out that many experiments are, in fact, consistent with this proposal and discussed how signals of the first transition, from the BG to the MG phase, may often be hard to detect. We have also presented a simple analytic parametrization for the BG-MG phase boundary, drawing on earlier work [8,9] as well as provided an analytical expression for the MG-DL phase boundary. These are consistent with the experimental data.

Hypothesizing a multi-domain state in the intermediate- H regime is consistent with the experimental data. This suggestion rationalizes the association of thermodynamic melting with the MG-DL transition line; for a prior suggestion in this regard see Ref. [24]. In addition, given the expectation that the effects of disorder increase as H increases, it indicates a physical mechanism for the occurrence of a critical point on the first-order MG-DL transition line.

Related theoretical and simulation work which bears on ideas proposed here include work by Feinberg [120], Ikeda [119] and van Otterlo *et. al.*. Ikeda has suggested that a vortex glass instability may accompany a first-order solidification transition in the presence of weak point pinning disorder [119]. Feinberg has argued that melting of the Bragg glass may be to an intermediate glassy phase, *via* a reentrance of single particle pinning [120]. van Otterlo *et. al.* point out that their simulation work cannot rule out the possibility of a sliver of glassy phase always intervening between ordered and fluid phases, as in the phase

diagram of Fig. 2. Several authors have commented [123], on the relation of these simulation results to their experimental data. Some of the ideas presented here also have overlaps with recent work by Kierfeld and Vinokur [24]. A recent comprehensive survey of the status of vortex glass phases [11] makes much the same points as we do regarding the absence of a true phase-coherent MG phase as envisaged in the original proposal [6]. Several of the ideas presented here draw from extensive work on peak effect phenomena in 2H-NbSe₂ and related materials, summarized in Ref. [34].

Many of the proposals presented here are, in fact, experimentally testable. One is our proposal of a multi-domain phase. Experiments which probe local correlations should be able to access such structure. We have suggested that in the regime where the sliver of intervening glassy phase narrows, structural correlations in this intermediate phase should become large. This proposal is testable both in simulations and in experiments.

The second is our identification of the first of the two phase transitions out of the BG phase on increasing T as a thermodynamic phase transition. Signals of this phase transition in the form of entropy jumps or singularities in the specific heat will be extremely small, since they reflect ordering at the scale of units of 10^4 vortex lines or more. However, it remains to be seen whether high-precision experiments might be able to resolve our suggestion of *two* equilibrium, thermodynamic phase transitions generically separating the low temperature Bragg glass phase from the disordered liquid. Such experiments would provide crucial evidence in favour of the ideas presented here.

Perhaps the single most novel proposal of this paper is the conjecture that the low- T , quasi-lattice Bragg glass phase in *all* superconductors should generically melt into an intermediate glassy phase before finally transforming into a liquid [57]. This possibility violates none of what is known about the phenomenology of the experimental data, nor the simulations nor available theoretical evidence. Further tests of the ideas presented here as well as first-principles calculations of the phase diagram of Fig. 2 would be very welcome.

VIII. ACKNOWLEDGEMENTS

I thank my coauthors on Ref. [35] – S.S. Banerjee, T.V. Chandrasekhar Rao, A.K. Grover, M.J. Higgins, P.K. Mishra, D. Pal, S. Ramakrishnan, G. Ravikumar, V.C. Sahni, S. Sarkar and C.V. Tomy. I thank Deepak Dhar and G. Ravikumar for useful discussions. I am grateful to C. Dasgupta for a critical reading of the manuscript and for many clarifying discussions. A useful conversation with S. Sondhi is acknowledged. This work evolved out of many discussions with S. Bhattacharya – he exerted a profound influence in shaping the ideas presented here. The author is partially supported by a DST (India) Fast Track Fellowship for Young Scientists.

REFERENCES

- [1] G. Blatter, M.V. Feigel'man, V.B. Geshkenbein, A.I. Larkin and V.M. Vinokur, *Rev. Mod. Phys.* **66**, 1125 (1994).
- [2] D. R. Nelson, *Phys. Rev. Lett.* **60**, 1973 (1988).
- [3] A. Houghton, R.A. Pelcovits and A. Sudbo, *Phys. Rev. B*, **40**, 6763 (1989).
- [4] S. Sengupta, C. Dasgupta, H. R. Krishnamurthy, G. I. Menon and T. V. Ramakrishnan, *Phys. Rev. Lett.* **67**, 3444 (1991); G.I. Menon, C. Dasgupta, H.R. Krishnamurthy, T.V. Ramakrishnan and S. Sengupta, *Phys. Rev. B*, **54**, 16192 (1996).
- [5] A.I. Larkin, *Sov. Phys. JETP*, **31**, 784 (1970).
- [6] D. S. Fisher, M. P. A. Fisher and D. A. Huse, *Phys. Rev. B* **43** 130 (1991).
- [7] T. Nattermann, *Phys. Rev. Lett.* **64**, 2454 (1990).
- [8] T. Giamarchi and P. Le Doussal, *Phys. Rev. Lett.* **72**, 1530 (1994); *Phys. Rev. B*, **52**, 1242 (1995).
- [9] T. Giamarchi and P. Le Doussal, *Phys. Rev. B*, **55**, 6577 (1997).
- [10] M. J. P. Gingras and D. A. Huse, *Phys. Rev. B* **53** 15193 (1996).
- [11] T. Natterman and S. Scheidl, *Advances in Physics*, **49**, 607, (2000).
- [12] T. Emig, S. Bogner and T. Natterman, *Phys. Rev. Lett.* **83**, 400, (2000).
- [13] D. Grier *et. al.*, *Phys. Rev. Lett.* **66**, (1991) 2270.
- [14] R. Cubitt *et al.*, *Nature* **365**, 407 (1993)
- [15] E. Zeldov, D. Majer, M. Konczykowski, V.B. Geshkenbein, V.M. Vinokur, H. Shtrikman, *Nature*, **375**, 373 (1995).
- [16] P.L. Gammel, D.A. Huse and D.J. Bishop, in *Spin Glasses and Random Fields*, ed.

A.P. Young, (World Scientific, Singapore), (1998) pp. 229.

[17] T. Giamarchi and P. Le Doussal, in Ref. [16] pp. 321.

[18] There is experimental evidence that the DL-MG transition is accompanied by a substantial increase of relaxation times, see e.g. S. Misat, P.J. King, R.P. Campion, P.S. Czerwinka, D. Fuchs and J.C. Villegier, *J. Low Temp. Phys.*, **117** 1381 (1999). Pronounced history dependence is also seen in the MG phase, see e.g. S. Kokkaliaris, A.A. Zhukov, S.N. Gordeev, P.A.J. de Groot, R. Gagnon and L. Taileffer *J. Low Temp. Phys.*, **117** 1341 (1999); A.P. Rassau, S.N. Gordeev, P.A.J. de Groot, R. Gagnon and L. Taileffer, *Physica B*, 284-288 693 (2000); M. Konczykowski, S. Colson, C.J. van der Beek, M.V. Indenbom, P.H. Kes and E. Zeldov, *Physica C* **332** 219 (2000); D. Giller, A. Shaulov, R. Prozorov, Y. Abulafia, Y. Wolfus, L. Burlachkov, Y. Yeshurun, E. Zeldov, V.M. Vinokur, J.L. Peng and R.L. Greene, *Phys. Rev. Lett.*, **79**, 2542 (1997).

[19] See C. Dasgupta and G.I. Menon, in *Studies of High-Temperature Superconductors - Vol 31*, ed. A.V. Narlikar (Nova Science Publishers, New York) (2000) p 33.

[20] V. Vinokur, B. Khaykovich, E. Zeldov, M Konczykowski, R.A. Doyle and P.H. Kes, *Physica C*, **295**, 209, (1998).

[21] G. I. Menon, C. Dasgupta and T.V. Ramakrishnan, *Phys. Rev. B*, **60** 7607 (1999).

[22] D. Ertaz and D. R. Nelson, *Physica C* **272** 79 (1996).

[23] J. Kierfeld, *Physica C*, **300**, 171, (1998).

[24] J. Kierfeld and V.M. Vinokur, *Phys. Rev. B*, **61**, R14928, (2000).

[25] The dominant source of disorder in these crystals is localized pinning sites such as vacancies or interstitials in the host crystal.

[26] We will thus discuss data on systems where pinning by extended defects such as lattice dislocations, grain boundaries, twins or ion tracks is absent.

[27] G. I. Menon and C. Dasgupta, *Phys. Rev. Lett.* **73** 1023 (1994).

[28] M.B. Gaifullin, N. Chikumoto, J. Shimoyama and K. Kishio, *Phys. Rev. Lett.*, **84**, 2945, (2000).

[29] C.J. van der Beek, S. Colson, M.V. Indenbom and M. Konczykowski *Phys Rev. Lett.*, **84**, 4196, (2000).

[30] Y. Nonomura and X. Hu, (preprint <http://arXiv.org/abs/cond-mat/0002263>)

[31] S. S. Banerjee, S. Saha, N. G. Patil, S. Ramakrishnan, A. K. Grover, S. Bhattacharya, G. Ravikumar, P. K. Mishra, T. V. C. Rao, V. C. Sahni, C. V. Tomy, G. Balakrishnan, D. Mck. Paul, M. J. Higgins, *Physica C*, **308** 25 (1998).

[32] S. S. Banerjee, N. G. Patil, S. Ramakrishnan, A. K. Grover, S. Bhattacharya, G. Ravikumar, P. K. Mishra, T. V. C. Rao, V. C. Sahni, M. J. Higgins, C. V. Tomy, G. Balakrishnan and D. McK Paul, *Phys. Rev. B* **59** 6043 (1999).

[33] S. S. Banerjee, N. G. Patil, S. Saha, S. Ramakrishnan, A. K. Grover, S. Bhattacharya, G. Ravikumar, P. K. Mishra, T. V. Chandrasekhar Rao, V. C. Sahni, M. J. Higgins, E. Yamamoto, Y. Haga, M. Hedo, Y. Inada and Y. Onuki, *Phys. Rev. B* **58**, 995 (1998).

[34] S. S. Banerjee, S. Ramakrishnan, D. Pal, S. Sarkar, A. K. Grover, G. Ravikumar, P. K. Mishra, T. V. C. Rao, V. C. Sahni, C. V. Tomy, M. J. Higgins and S. Bhattacharya, *J. Phys. Soc. Jpn. Suppl.* **69** 262 (2000).

[35] S.S. Banerjee, T.V.C. Rao, A.K. Grover, M.J. Higgins, G. I. Menon, P.K. Mishra, D. Pal, S. Ramakrishnan, G. Ravikumar, V.C. Sahni, S. Sarkar and C.V. Tomy, preprint (<http://arXiv.org/abs/cond-mat/0007451>) (to appear in *Physica C*).

[36] M. J. Higgins and S. Bhattacharya, *Physica C* **257** 232 (1996) and references cited therein.

[37] S. Bhattacharya and M.J. Higgins, *Phys. Rev. B*, **49**, 10005 (1994); *Phys. Rev. B*, **52**,

64 (1995); *Phys. Rev. Lett.*, **70**, 2617 (1993).

[38] S.B. Roy, P. Chaddah and S. Chaudhury, *J. Phys. Cond. Matt.*, **10**, 4885, (1998); See S.B. Roy and P. Chaddah, *Pramana*, **53**, 659, (1999) and references therein.

[39] C. V. Tomy, G. Balakrishnan and D. Mck. Paul, *Physica C* **280** 1, (1997).

[40] C. V. Tomy, G. Balakrishnan and D. McK. Paul, *Phys. Rev. B* **56** 8346 (1997).

[41] S. Sarkar, D. Pal, S. S. Banerjee, S. Ramakrishnan, A. K. Grover, C. V. Tomy, G. Ravikumar, P. K. Mishra, V. C. Sahni, G. Balakrishnan, D. Mck. Paul and S. Bhattacharya, *Phys. Rev. B* —bf 61, 12394, (2000).

[42] K. Hirata, H. Takeya, T. Mochiku and K. Kadowaki, in *Advances in Superconductivity VIII*, ed by H. Hayakawa and Y. Enomoto (Springer-Verlag, Berlin, Germany, 1996) p. 619.

[43] D. Lopez *et. al.*, *Phys. Rev. Lett.*, **80**, 1070, (1998).

[44] In contrast, the transition to the vortex glass phase was *assumed* to be continuous in Ref. [6]. These authors ignored spatial correlations in the resulting phase, in effect assuming that such correlations were extremely short-ranged.

[45] J. Kierfeld, H. Nordborg and V.M. Vinokur, *Phys. Rev. Lett.*, **85**, 4948 (2000).

[46] A. Soibel, E. Zeldov, M. Rappaport, Y. Myasoedov, T. Tamegai, S. Ooi, M. Konczykowski and V.B. Geshkenbein, *Nature*, **406**, 282, (2000)

[47] R. Merithew, M. W. Rabin and M. B. Weismann, M. J. Higgins and S. Bhattacharya, *Phys. Rev. Lett.* **77** 3197 (1996).

[48] S. Ooi, T. Shibauchi and T. Tamegai, *Physica B*, **284-288**, 775, (2000).

[49] S. Bhattacharya, *private communication*.

[50] Some of the possibilities for the topologies of the transition lines in such a case are

illustrated in Ref. [16].

- [51] K. Ghosh, S. Ramakrishnan, A. K. Grover, G. I. Menon, G. Chandra, T. V. C. Rao, G. Ravikumar, P. K. Mishra, V. C. Sahni, C. V. Tomy, G. Balakrishnan, D. Mck Paul and S. Bhattacharya, *Phys. Rev. Lett.*, **76**, 4600 (1996).
- [52] D. Pal, D. Dasgupta, B.K. Sarma, S. Bhattacharya, S. Ramakrishnan and A.K. Grover, *Phys. Rev. B*, **62**, 6299, (2000).
- [53] C. Hucho, J.M. Carter, V. Muller, A. Petrean and W.K. Kwok, *Physica C*, **332**, 370, (2000).
- [54] D. R. Nelson and P. Le Doussal, *Phys. Rev. B* **42**, 10133 (1990).
- [55] W. Magro and D.M. Ceperley, *Phys. Rev. Lett*, **73**, 826, (1994); *Phys. Rev. B*, **48**, 411, (1993).
- [56] Y. Paltiel, E. Zeldov, Y. N. Myasoedov, H. Shtrikman, S. Bhattacharya, M. J. Higgins, Z. L. Xiao, E. Y. Andrei, P. L. Gammel and D. J. Bishop, *Phys. Rev. Lett*, **85**, 3712 (2000).
- [57] G.I. Menon, *Phase Transitions*, to appear.
- [58] T.G. Belincourt, R.R. Hake and D.H. Leslie, *Phys. Rev. Lett*, **6**, 671, (1961).
- [59] A.M. Campbell and J.E. Evertts, *Advan. Phys.*, **21**, 199, (1972); M. Steingart, A.G. Putz and E.J. Kramer, *J. Appl. Phys*, **44**, 5580, (1973)
- [60] P.H. Kes and C.C. Tsuei, *Phys. Rev. Lett.*, **47**, 1930, (1981); *Phys. Rev. B*, **28**, 5126, (1983).
- [61] X.S. Ling, J.E. Berger and D.E. Prober, *Phys. Rev. B*, **57**, R3249, (1998).
- [62] S. S. Banerjee, N. G. Patil, K. Ghosh, S. Saha, G. I. Menon, S. Ramakrishnan, A. K. Grover, P. K. Mishra, T. V. C. Rao, G. Ravikumar, V. C. Sahni, C. V. Tomy, G.

Balakrishnan, D. Mck. Paul and S. Bhattacharya, *Physica B* **237-238**, 315 (1997).

[63] A. I. Larkin and Yu. N. Ovchinnikov, *Sov. Phys. JETP* **38** 854 (1974); *J. Low Temp. Phys.* **34** 409 (1979).

[64] Y. Paltiel, E. Zeldov, Y. N. Myasoedov, H. Shtrikman, S. Bhattacharya, M. J. Higgins, Z. L. Xiao, E. Y. Andrei, P. L. Gammel and D. J. Bishop, *Nature* **403** (2000) 398.

[65] H.S. Bokil and A.P. Young, *Phys. Rev. Lett.* **74**, 3021, (1995); C.Wengel and A.P. Young, *Phys. Rev B*, **54**, R6869, (1996) F.O. Pfeiffer and H. Rieger, *Phys. Rev. B*, **60**, 6304, (1999); H. Kawamura, *J. Phys. Soc. Jpn.*, **69**, 29, (2000).

[66] D.R. Strachan, M.C. Sullivan, P. Fournier, S.P.Pai, T. Venkatesan and C.J. Lobb, *cond-mat/0011014*.

[67] B. Brown, *Phys. Rev. B*, **61**, 3267, (2000).

[68] W. Henderson, E. Y. Andrei, M. J. Higgins and S. Bhattacharya, *Phys. Rev. Lett.* **77**, 2077 (1996).

[69] A.C. Marley, M.J. Higgins and S. Bhattacharya, *Phys. Rev. Lett.* **74**, 3029, (1995).

[70] W. Henderson, E.Y. Andrei and M.J. Higgins, *Phys. Rev. Lett.* **81**, 2352, (1998).

[71] Recent work which models a structural glass transition in particle systems without quenched disorder suggests an unambiguous way, based on a replica treatment, by which a structural glass may be distinguished from the liquid; see M. Mezard and G. Parisi, *J. Phys. A*, **29**, 6515, (1996). Connections to the vortex phase diagram are suggested in F. Thalmann, C. Dasgupta and D. Feinberg, *Europhys. Lett.* **50**, 54, (2000) and in C. Dasgupta and O.T. Valls, preprint <http://arXiv.org/abs/cond-mat/0002186>.

[72] S. S. Banerjee, N. G. Patil, S. Ramakrishnan, A. K. Grover, S. Bhattacharya, G. Ravikumar, P. K. Mishra, T. V. Chandrasekhar Rao, V. C. Sahni, M. J. Higgins, *Appl. Phys. Lett.* **74**, 126 (1999).

[73] X.S. Ling, S.R. Park, B.A. MaClain, S.M. Choi, D.C. Dender and J.W. Lynn, *Phys. Rev. Lett.*, **86**, 712, (2001).

[74] T. Blasius, Ch. Niedermayer, J.L. Tallon, D.M. Pooke, A. Golnik and C. Bernhard, *Phys. Rev. Lett.*, **82**, 4296, (1999).

[75] J. Sonier, J. Brewer and R.F. Kiefl, *Rev. Mod. Phys.*, **72**, 769 (2000).

[76] T. Nishizaki and N. Kobayashi, *Supercon. Sci. Tech.*, **13**, 1, (2000);

[77] T. Nishizaki, T. Naito, and N. Kobayashi, *Phys. Rev. B*, **58**, 11169 (1998).

[78] S.N. Gordeev, D. Braconovic, A.P. Rassau, P.A.J. de Groot, R. Gagnon and L. Taileffer *Phys. Rev. B*, **57**, 645, (1998).

[79] A.P. Rassau, S.N. Gordeev, P.A.J. de Groot, R. Gagnon and L. Taileffer, *J. Low Temp. Phys.*, **117**, 1507, (1999).

[80] C.J. Olson, C. Reichhardt, R.T. Scalettar, G.T. Zimanyi and N. Gronbech-Jensen, preprint <http://arXiv.org/abs/cond-mat/0008350>.

[81] A. van Otterlo, R.T. Scalettar and G.T. Zimanyi, *Phys. Rev. Lett.*, **81**, 1497, (1998).

[82] A van Otterlo, R.T. Scalettar, G.T. Zimanyi, R. Olsson, A. Petrean, W. Kwok and V. Vinokur, *Phys. Rev. Lett.*, **84**, 2493, (2000)

[83] K. Binder and A.P. Young, *Rev. Mod. Phys.* **58**, 801 (1986); M. Mezard, G. Parisi and M.A. Virasoro eds., *Spin Glass Theory and Beyond* (World Scientific, Singapore, 1987).

[84] A.B. Pippard, *Philos. Mag.*, **19**, 217, (1969).

[85] E. M. Chudnovsky, *Phys. Rev. Lett.* **65**, 3060 (1990).

[86] T. Nishizaki, K. Shibata, T. Naito, M. Maki and N. Kobayashi, *J. Low. Temp. Phy.*, **117**, 1375, (1999); T. Nishizaki, K. Shibata, T. Sasaki and N. Kobayashi, in *Proceedings*

of the 6th International Conference on Materials and Mechanisms of Superconductivity and High-Temperature Superconductors - 2000.

- [87] B. Billon, M. Charalambous, J. Chaussy, R. Koch, and R. Liang, *Phys. Rev. B*, **55**, R14753, (1997).
- [88] D. Majer, E. Zeldov and M. Konczykowski, *Phys. Rev. Lett.*, **75**, 1166, (1995).
- [89] W.E. Lawrence and S. Doniach, in: *Proc. Twelfth International Conf. on Low Temperature Physics*, E. Kanda ed. (Keigaku, Tokyo, 1971).
- [90] J.P. Hansen and D. R. Macdonald, *Theory of Simple Liquids*, (Academic Press. London, 1986), 2nd edition.
- [91] T. V. Ramakrishnan and M. Yussouff, *Phys. Rev. B* **19**, 2775 (1979).
- [92] C. P. Bean, *Phys. Rev. Lett.* **8** (1962) 250.
- [93] V.N. Kopylov, I.F. Schegolev and T.G. Tonidze, *Physica C*, **162-164**, 1143, (1989)
- [94] M. Daeumling, J.M. Seuntjens and D.C. Larbalestier, *Nature* (London), **346**, 332, (1990).
- [95] N. Chikumoto, M. Konczykowski, N. Motohira. K. Kishio and K. Kitazawa, *Physica C*, **185-189**, 2201, (1991).
- [96] B. Khaykovich, E. Zeldov, D. Majer, T.W. Li, P.H. Kes and M. Konczykowski, *Phys. Rev. Lett.*, **76**, 2555, (1996).
- [97] In BSCCO, the fishtail effect is a spectacular and sharp feature, immediately suggesting a link to an underlying thermodynamic phase transition [96]. In YBCO and less anisotropic high- T_c materials, the onset of the fishtail feature is more gradual and the association to an underlying equilibrium transition more indirect.
- [98] D. Giller, A. Shaulov, Y. Yeshurun and J. Giapintzakis, *Phys Rev. B*, **60**, 106, (1999).

[99] G. Ravikumar, P.K. Mishra, V.C Sahni, S.S. Banerjee, S. Ramakrishnan, A.K. Grover, P.L. Gammel, D.J. Bishop, E. Bucher, M.J. Higgins and S. Bhattacharya, *Physica C* (to appear).

[100] M. Saalfrank, M. Niderost, A.C. Mota and P. Kes, *Physica B*, **284-288**, 549, (2000).

[101] H.J. Jensen, A. Brass and A.J. Berlinsky, *Phys Rev. Lett*, **60**, 1676, (1988); A-C. Shi and J. Berlinsky, *Phys. Rev. Lett.* **67**, 1926, (1991); M.C. Faleski, M.C. Marchetti and A.A. Middleton, *Phys. Rev. B*, **54**, 12427, (1996).

[102] K. Tenya, S. Yasunami, T. Tayama, H. Amitsuka, T. Sakakibara, M. Hedo, Y. Inada, E. Yamamoto, Y. Haga and Y. Onuki, *J. Phys. Soc. Jpn.*, **68**, 224, (1999).

[103] The possibility of a first-order transition in the mixed phase was suggested, given the existence of slight hysteretic effects, a mild discontinuity in the specific heat and somewhat more unequivocal thermo-mechanical signals. However, no magnetization discontinuity was seen.

[104] The MG phase has a density which differs from that of the fluid. There is no *a-priori* reason why the liquid-liquid transition should necessarily coincide with the transition into the glass. Fig. 4 of Ref. [57] addresses such a possibility.

[105] Y. Abulafia, A. Shaulov, Y. Wolfus, R. Prozorov, L. Burlachkov, Y. Yeshurun, D. Majer, E. Zeldov, H. Wuhl, V.B. Geshkenbein and V.M. Vinokur, *Phys. Rev. Lett*, **77**, 1596 (1997).

[106] T. Klein, W. Harneit, L. Baril, C. Escribe-Filippini and D. Feinberg, *Phys. Rev. Lett*, **79**, 3795 (1997).

[107] Y. Abulafia, A. Shaulov, Y. Wolfus, R. Prozorov, L. Burlachkov, Y. Yeshurun, D. Majer, E. Zeldov, H. Wuhl, V.B. Geshkenbein and V.M. Vinokur, *Phys. Rev. Lett*, **79**, 3796 (1997).

[108] G. d'Anna, P.L. Gammel, H. Safar, G.B. Alers, D.J. Bishop, J. Giapintzakis and D.M. Ginsberg, *Phys. Rev. Lett.*, **75**, 3521, (1995).

[109] A.D. Huxley, C. Paulsen, O. Laborde, J.L. Tholence, D. Sanchez, A. Junod and R. Calemzuk, *J. Phys. Cond. Matt.*, **5**, 7709, (1993).

[110] P. Fulde and R. A Ferrell, *Phys. Rev.*, **135**, 550, (1964); A.I. Larkin and Y.N. Ovchinnikov, *Zh. Eksp. Teor. Fiz.*, **47**, 1136, (1964)[Sov. Phys. JETP **20**, 762, (1965)].

[111] M. Tachiki, S. Takahashi, P. Gegenwart, M. Weiden, M. Lang, C. Geibel, F. Steglich, R. Modler, C. Paulsen and Y. Onuki, *Z. Phys. B*, **100**, 369, (1996).

[112] H. Sato, Y. Kobayashi, H. Sugawara, Y. Aoki, R. Settai and Y. Onuki, *J. Phys. Soc. Jpn.*, **65**, 1536, (1996).

[113] N.R. Dilley, J. Herrmann, S.H. Han, M.B. Maple, S. Spagna, J. Diderichs and R.E. Sager, *Physica C*, **265**, 150, (1996).

[114] A. Yamashita, K. Ishii, T. Yokoo, J. Akemitsu, M. Hedo, Y. Inada, Y. Onuki, E. Yamamoto, Y. Haga and Y. Kadono, *Phys. Rev. Lett.*, **79**, 3771, (1997).

[115] G. d'Anna, M.V. Indenbom, M.O. Andre, M. Benoit, E. Walker, *Europhys. Lett.*, **25**, 225, (1994); *ibid.* **25**, 539, (1994).

[116] T. Ishida, K. Okuda and H. Asaoka, *Phys. Rev. B*, **56**, 5128, (1997).

[117] J. Shi, X.S. Ling, R. Liang, D.A. Bonn and W.N. Hardy, *Phys. Rev. B*, **60**, R12593, (1999).

[118] D. Giller, A. Shaulov, R. Prozorov, Y. Abulafia, Y. Wolfus, L. Burlachkov, Y. Yeshurun, E. Zeldov, V.M. Vinokur, J.L. Peng, R.L. Greene, *Phys. Rev. Lett.*, **79**, 2542, (1997).

[119] R. Ikeda, *J. Phys. Soc. Jpn.*, **65**, 3998, (1996);

- [120] D. Feinberg, <http://xxx.lanl.gov/abs/cond-mat/9805080>
- [121] M. Pissas, E. Moraitakis, G. Kallias and A. Bondarenko, *Phys. Rev. B*, **62**, 1446, (2000).
- [122] A. Rydh, M. Andersson and O. Rapp, *J. Low Temp. Phys.*, **117**, 1335, (1999).
- [123] T. Klein, A. Conde-Gallardo, J. Marcus, C. Escrie-Filippini, P. Samuely, P. Szabo and A.G.M. Jansen, *Phys. Rev. B*, **58**, 12411, (1998); T. Klein, I. Journard, J. Marcus and R. Cubitt, *J. Low Temp. Phys.*, **117**, 1353, (1999); I. Journard, T. Klein, J. Marcus and R. Cubitt, *Phys. Rev. Lett*, **82**, 4930, (1999).
- [124] S. Ooi, T. Shibauchi and T. Tamegai, **Physica C**, **302**, 339, (1998).
- [125] R. Sugano, T. Onogi, K. Hirata and M. Tachiki, *Physica B*, **284-288**, 803, (2000); R. Sugano *et. al.* *Phys. Rev. Lett*, **80**, 2925, (1998).

FIGURES

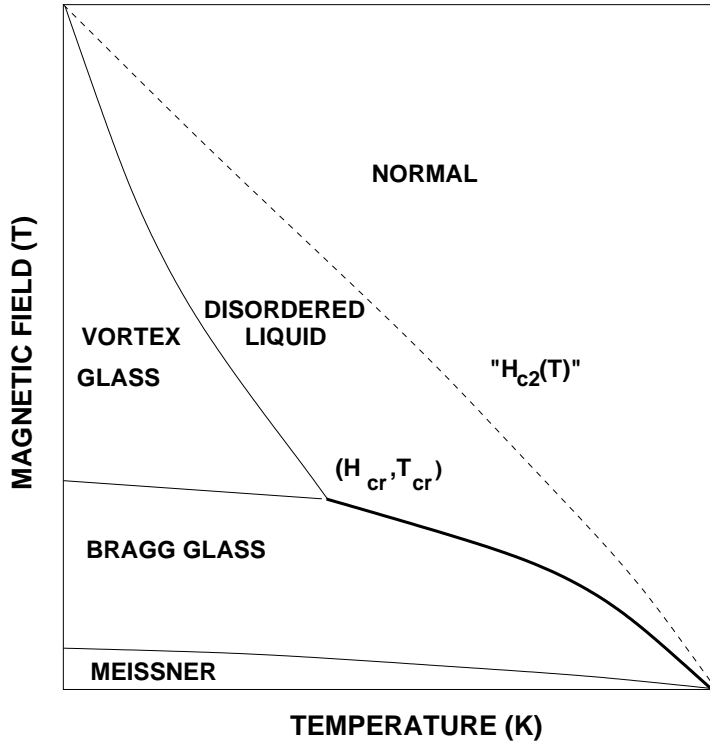


FIG. 1. The current view of the phase diagram of type-II superconductors [9,17,16,11,20,24], incorporating the effects of quenched disorder and thermal fluctuations. In addition to Meissner and normal phases, this phase diagram subdivides the mixed phase into three phases – the Bragg glass (BG), the vortex glass (VG) and the disordered liquid (DL). The BG melts directly into the DL phase through a first-order melting transition on T scans at intermediate H . On H scans at fixed low T , the BG phase transforms discontinuously [28,29] into the disordered VG phase. The VG phase is understood to transform via a continuous phase transition, with the exponents linked by relations calculated in Ref. [6], into the DL phase. This line of continuous phase transitions meets the BG phase boundary at a “multicritical” point, labelled (H_{cr}, T_{cr}) in the figure. The first-order direct transition from BG to DL may persist beyond the putative (H_{cr}, T_{cr}) [43,77,24] terminating in a critical point (not shown in this figure, see Refs. [24,11]). The line which separates the DL from the normal phase is a crossover line and not a true phase transition. This phase diagram does not show the small regime of reentrant glassy phase expected at low field values; for a phase diagram which includes this see Ref. [11].

FIG. 2. Proposed universal phase diagram for type-II superconductors incorporating the effects of thermal fluctuations and quenched random point pinning. The term multi-domain glass (MG) is used here in preference to “vortex glass”; for a discussion of this point and of the properties of this phase, see text. The other phases are described in the caption of Fig. 1. Note that the MG phase intrudes between BG and DL phases everywhere in the phase diagram. At intermediate H where interactions dominate, the MG phase is confined to a slim sliver but broadens out again for sufficiently low H . The putative “multicritical point” (H_{cr}, T_{cr}) of Fig. 1 is identified with the location where the BG-MG and MG-DL transition line first approach so closely that they cannot be separately resolved. The inset to the figure expands the boxed region shown in the main panel at low fields and temperature values close to $T_c(0)$ and illustrates the reentrant nature of the BG-MG phase boundary at low fields. The transition line separating the MG from the DL phase is first order at low fields but terminates at a tricritical point, where it meets a line of (equilibrium) glass transitions. The transition out of the BG phase is generically first-order.

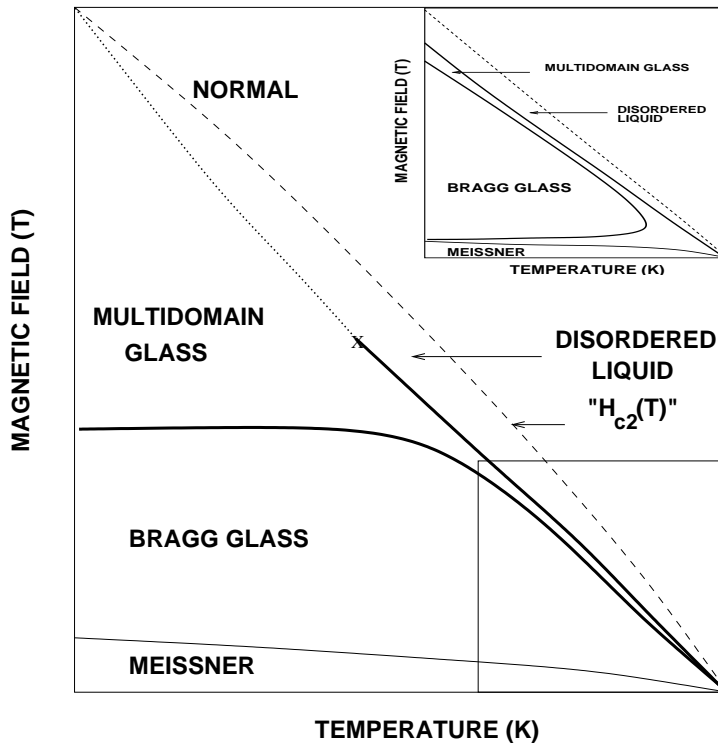


FIG. 3. Plot of Eq. 3.14, the expression for the BG-MG phase boundary in the b, t plane (b and t are the reduced field and temperature H/H_{c2} and T/T_c respectively), derived in Sec. III, for different values of Σ , in the range $0.01 < \Sigma < 60$ (see text). Σ is a phenomenological fitting parameter involving the Lindemann parameter and fundamental constants.

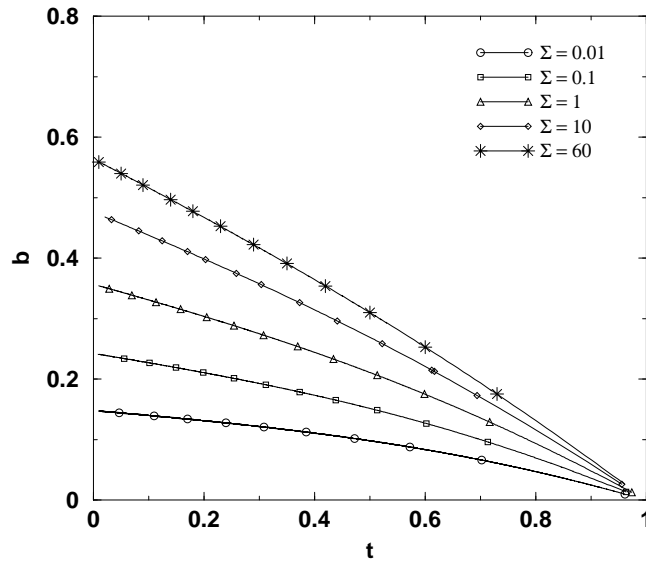


FIG. 4. Plot of Eq. 3.17, the expression for the BG-MG phase boundary in the b, t plane (b and t are the reduced field and temperature H/H_{c2} and T/T_c respectively), derived in Sec. III, for different values of Σ , in the range $0.01 < \Sigma < 60$ (see text). Σ is a phenomenological fitting parameter involving the Lindemann parameter and fundamental constants.

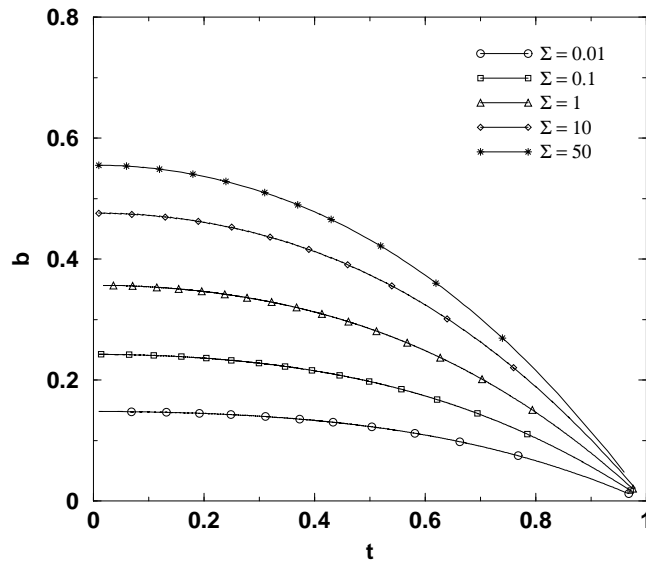


FIG. 5. Plot of Eq. 4.14, the expression for the MG-DL phase boundary incorporating the effects of quenched disorder as described in the text, derived in Sec. IV. The data use a T_c value of 7K, as appropriate for 2H-NbSe₂, a prefactor C of 1.15 kG (chosen purely for illustrative purposes) and values of $Cm = 0, 0.3$ and 0.5 . Note that the pure melting line is increasing suppressed by quenched disorder, this suppression becoming larger as the applied field H is increased, in agreement with the predictions of Ref. [27] and experiments.

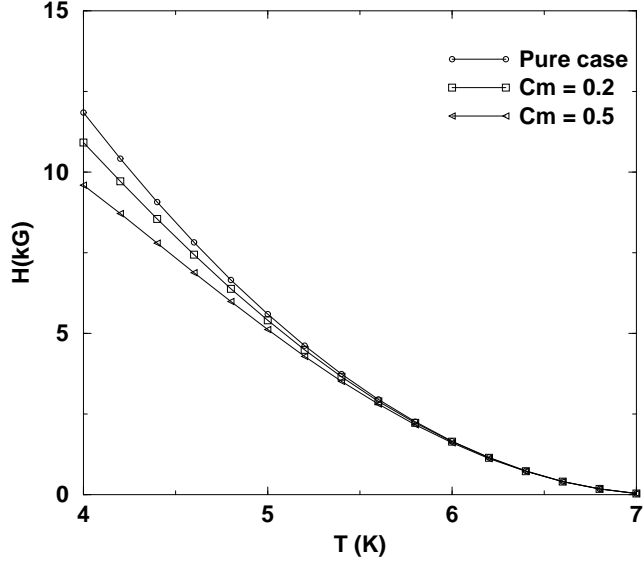


FIG. 6. Plot of the experimental data for (H_{pl}, t_{pl}) in single crystals of 2H-NbSe₂ (points taken from Fig. 2(a) of Ref. [34]) together with a best fit line based on Eqn.(3.14). Here t_{pl} is T_{pl}/T_c . An upper critical field of $H_{c2}(0) = 46$ kG is assumed in the normalization of b and $\Sigma = 60$ is used; see text.

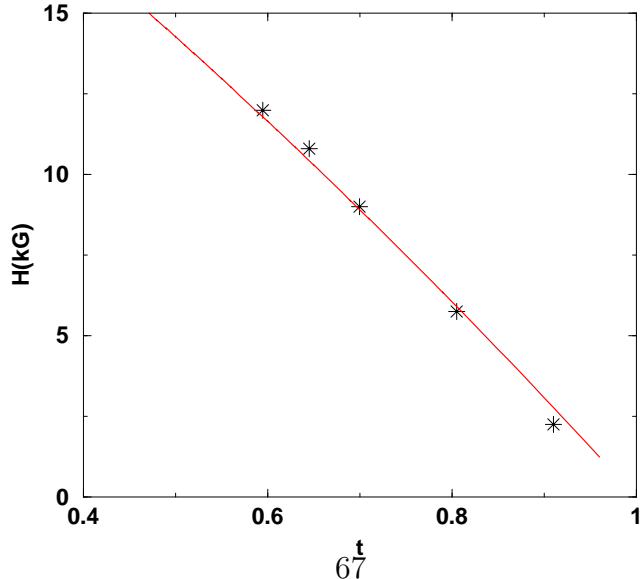


FIG. 7. Data points representing the BG-MG phase boundary in CeRu₂ (points taken from plots of (H_{pl}, T_{pl}) in Fig. 3(b) of Ref. [31]), together with a best fit based on Eqn.(3.17). An upper critical field of 68kG and a T_c of 6.2 K is assumed in the normalization of the y -axis. A value of $\Sigma = 0.01$ is used; see text.

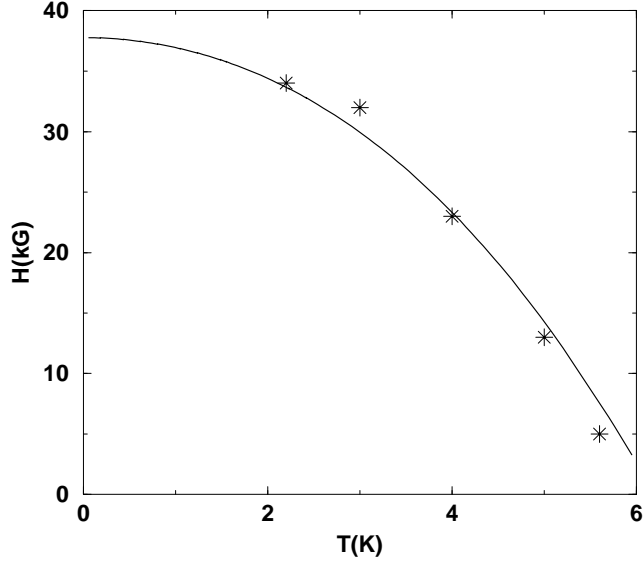


FIG. 8. Data points obtained from plots of H_{pl}, t_{pl} in Ca₃Rh₄Sn₁₃ (from Fig. 3(c) of Ref. [34]) are shown together with best fits based on Eqn.(3.14. An upper critical field H_{c2} of 45 kG is assumed in the normalization of the y -axis in the comparison to experimental data. A value of $\Sigma = 0.01$ is used; see text.

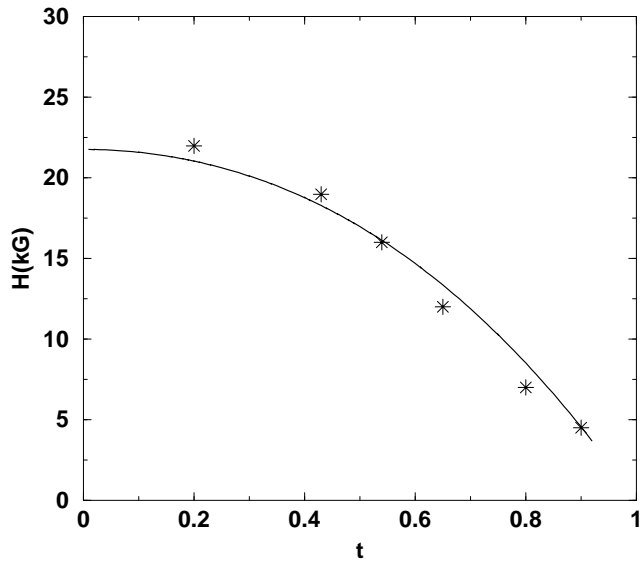


FIG. 9. The solid line is the solution of Eq.3.17 with $\Sigma = 0.001$. The dotted line is the fitting form $B_m = B_0(1 - (T/T_c)^4)^{3/2}$, which provides an accurate fit to the onset value of the fishtail effect in NCCO [118]. The prefactors are chosen to allow the two curves to overlap as extensively as possible.

